

States of the ^{12}C Nucleus in the Toroidal Configuration

Cheuk-Yin Wong*

Physics Division, Oak Ridge National Laboratory, Oak Ridge, TN 37831, USA

Andrzej Staszczak†

*Institute of Physics, Maria Curie-Skłodowska University,
pl. M. Curie-Skłodowskiej 1, 20-031 Lublin, Poland*

(Dated: January 15, 2022)

The ^{12}C nucleus with $N=6$ and $Z=6$ is a doubly closed-shell nucleus in a toroidal potential. In the description of the ground state and the Hoyle state of ^{12}C in the resonating group method or the generator coordinate method, a superposition of the orientations of Wheeler’s triangular cluster on the cluster plane would naturally generate an intrinsic toroidal density. A toroidal state also has a probability amplitude to overlap with a 3-alpha cluster, which is the dominant decay mode for the Hoyle state. For these reasons, we study a toroidal description of the states of ^{12}C in the toroidal configuration both phenomenologically and microscopically. A toroidal ^{12}C nucleus distinguishes itself by toroidal particle-hole multiplet excitations between one toroidal single-particle shell to another. From such a signature and experimental data, we find phenomenologically that the Hoyle state and many of its higher excited states may be tentatively attributed to those of the ^{12}C nucleus in a toroidal configuration. We then study the ^{12}C system from a microscopic mean-field approximation using variational wave functions. We find that the equidensity surfaces of the ^{12}C ground state exhibit a dense toroidal core immersed in lower-density oblate spheroids in the surface region. Furthermore, there are prominent toroidal features of the equidensity surfaces for the state at the Hoyle excitation energy, at which previous cluster model calculations indicate the presence of a 3-alpha cluster state. A toroidal coexistence model therefore may emerge to suggest the possibility that the physical Hoyle state may have probability amplitudes to be in the toroidal configuration and the 3-alpha cluster configuration, possessing features of both the toroidal particle-hole multiplet signature studied here and the 3-alpha cluster decay properties examined elsewhere.

PACS numbers: 21.10.Pc, 21.60.Cs

I. INTRODUCTION

The study of the intrinsic structure of the ^{12}C nucleus has a long history. Wheeler proposed an α particle model for α -conjugate nuclei and suggested in 1937 that the ^{12}C nucleus may be described as a triangular resonating grouping of three alpha clusters obeying Bose-Einstein statistics and exchanging nucleons between them [1, 2]. Later in 1953 Hoyle postulated an excited state of ^{12}C as the doorway for the triple alpha reaction in nucleosynthesis, in which two alpha particles fuse into beryllium-8 and then capture a third alpha particle to form the carbon-12 nucleus [3–5]. The excited 0^+ state at 7.654 MeV of ^{12}C was subsequently identified as the postulated “Hoyle state” [6]. Since then, many experimental and theoretical investigations have been carried out to understand the properties of the ^{12}C nucleus. Recent experimental and theoretical results and reviews have been presented in [7–26]. In addition to Wheeler’s α particle model for the ^{12}C nucleus, related theoretical models include the cluster model of Brink [27], the cluster model of three interacting alpha particles [23–26], the generator coordinate method [21, 28–30], the resonating group method [31–33], a Bose-Einstein condensate-type

cluster model [34–37], the (THSR) cluster wave function model [37], a Nilsson oblate ellipsoidal model [38] with a commensurate axis ratio of $a_\rho:a_z=2:1$ [39], an algebraic $U(7)$ model with a D_{3h} symmetry [40–42], an anti-symmetric molecular dynamics (AMD) model [43–46], a microscopic fermionic molecular dynamic (FMD) model [22, 47, 48], an *ab initio* no-core shell model [49, 50], a no-core simplectic model (NCSpM) [51], *ab initio* lattice effective field theory (L-EFT) [52], energy-density functional mean-field models [53–60], and a rod model of ^{12}C excited states [61–63]. For a review of microscopic cluster models, see Refs. [7, 19–22].

We study here the additional toroidal degree of freedom in the ^{12}C nucleus for many reasons. First and foremost is the reason that the physical nature of many excited states of ^{12}C has not been fully understood [7–21, 23–26]. On the other hand, Wheeler suggested that under appropriate conditions, a nucleus may assume a toroidal shape [64, 65]. Referring to toroidal nuclei and black holes, Wheeler wrote in his autobiography [65], “If nuclei could exist in doughnut shapes, I felt, then, some of them would exist in such shapes. If matter could collapse to infinitesimal or even zero size, then some matter would collapse. We physicists should think about where such extreme behavior might occur, and look for it.” A possible “extreme behavior” for a toroidal ^{12}C nucleus might be the presence of a strong toroidal shell effect, since the ^{12}C nucleus with $N=6$ and $Z=6$ is a doubly closed-shell

* wongc@ornl.gov

† andrzej.staszczak@poczta.umcs.lublin.pl

nucleus in the toroidal potential [66, 67]. The extrapolation from the toroidal nuclei results in Fig. 18 of Ref. [67], using the shell-correction method [68], points to a possible toroidal state in ^{12}C in the low excitation energy region. The “extreme behavior” of a strong shell effect in conjunction with the “extreme behavior” of a large yrast spin alignment lead to the prediction of a toroidal high-spin isomer in ^{28}Si [69], for which possible experimental observation has recently been presented [70]. Toroidal high-spin isomers under similar extreme behavior have also been predicted in the light-mass region from ^{24}Mg to ^{56}Ni in non-relativistic and relativistic mean-field theories [69, 71–76]. It is interesting to note that in the description of the ground state and the Hoyle state for the ^{12}C nucleus, a generator coordinate superposition of the orientations of Wheeler’s triangular cluster on the cluster plane would naturally generate an intrinsic toroidal density. A toroidal state also has a probability amplitude overlap with the state of three alpha particles, which is the dominant decay mode for the Hoyle state [14–18]. For all these reasons, it is of interest to follow Wheeler’s advice to think about where such extreme behavior for a toroidal nucleus might occur and look for it among states in the ^{12}C nucleus.

The 0^+ (ground) and $2^+(4.43\text{ MeV})$ states of the ^{12}C nucleus have been identified as members of the collective rotational band of a deformed nucleus with the quadrupole deformation parameter $\beta_2 = -0.6$ [77]. The intrinsic density of the nucleus with such a strongly negative quadrupole β_2 may contain both oblate spheroidal and toroidal equidensity surfaces. It is therefore useful to generalize the concept of the toroidal nucleus to include those for which *some* of its equidensity surfaces are toroidal.

In this first exploration of its kind to examine the toroidal degree of freedom of the ^{12}C nucleus, it is appropriate to study the problem from both the phenomenological and microscopic points of view. In the phenomenological study, we search for the signature of the ^{12}C nucleus in a toroidal configuration so as to facilitate its identification. The toroidal geometry of a toroidal nucleus is associated with distinctive properties of the single-particle states. The intrinsic shape of a toroidal ^{12}C nucleus shows up as a bunching of single-particle states into “ Λ -shells” whose spacing is intimately tied to the size of the toroidal major radius. This set of single-particle shells will generate a distinct pattern of particle-hole multiplet excitations that may be utilized to reveal the toroidal nature of the nucleus. We shall look for the possible occurrence of such a signature among the excited states of ^{12}C to explore phenomenologically whether the Hoyle state at 7.654 MeV may be the head of the toroidal band of the ^{12}C nucleus.

In the subsequent microscopic studies, we use the mean-field approximation and the Skyrme energy density functional to examine the energy of the system in many different shapes, ranging from the spherical, prolate spheroid, oblate spheroid, bi-concave disk, and toroidal density distributions. The investigation will be

carried out with variational single-particle wave functions characterized by a set of shape parameters. The energy as a function of the shape parameters provide useful information on the landscape of the energy surface and on the density distributions at different energy landscape points to facilitate the investigation on toroidal density distributions of the ground state and the state at the Hoyle excitation energy.

It is worth emphasizing at this point that while Wheeler’s concept of the ^{12}C nucleus as a triangular cluster of three alpha particles [1, 2] has been studied extensively in [21, 23–36], Wheeler’s other concept of possible toroidal nucleus [64, 65] has up to now not been applied to the ^{12}C nucleus, even though ^{12}C is a doubly closed-shell nucleus in a toroidal potential [66, 67]. Wheeler’s two different concepts should play their separate and important roles under different probes of the nucleus. In matters of 3α decay and the escape through the external Coulomb barrier, the 3α cluster description is clearly the simpler description. However, because nucleons can traverse azimuthal orbitals in a torus with low energies and can be excited to higher orbitals with a low excitation energies, a description in terms of a ^{12}C nucleus in toroidal doubly-closed shells may be an efficient description in matters associated with particle-hole excitations and in the energy spacing between particle-hole multiplet states. In contrast, the 3α cluster description has an unperturbed (one particle)-(one hole) energy excitation energy of order 20 MeV, and a large mixing of the many 3α determinants will be needed to bring the unperturbed levels down to the observed particle-hole excitation energy of a few MeV to about 10 MeV. Furthermore, the toroidal concept provides a novel geometrical insight, organizes useful concepts, helps guide our intuition, and may find many applications involving the ^{12}C nucleus. It is therefore beneficial to develop the toroidal concepts for the ^{12}C nucleus proposed here.

The paper is organized as follows. In Section II, we write down the approximate single-particle energies in a light toroidal nucleus which depend only on the effective toroidal major radius R and the orbital angular momentum component Λ_z along the symmetry z -axis. The method to calculate the quantum numbers and the excitation energies of the particle-hole excitations from these single-particle states are examined in Section III. The spectrum of ^{12}C in the toroidal configuration is investigated in Section IV. In Section V, we compare the theoretical predicted spectrum of toroidal states with observed ^{12}C states. In Section VI, we propose a toroidal constraint in mean-field dynamics to study the energy surface in the toroidal degree of freedom and to locate local energy minima in the toroidal configuration. In Section VII, we study the states of ^{12}C from a microscopic viewpoint using variational wave functions in terms of geometrical parameters. The search for the minimum of the energy using the Skyrme SkM* interactions [78–80] allows the determination of the ground state energy and density in Section VIII. We calculate the adiabatic en-

ergy surface and the density distributions for states above the ground state in Section IX. We examine the connection between the toroid and three-alpha cluster configurations. We study how a phenomenological toroidal co-existence model may emerge to contemplate the mixing of the toroidal and the three-alpha cluster descriptions of the ^{12}C states in Section X. In Section XI, we present our summary and discussions.

II. LOWEST SINGLE-PARTICLE STATES IN A TOROIDAL POTENTIAL

We consider a toroidal nucleus with an axially symmetric density distribution and choose the symmetry axis to be the z -axis. The nuclear density will generate an axially symmetric single-particle mean-field potential $V(\rho, z)$ that is independent of the azimuthal angle ϕ . The single-particle wave function of the lowest states for a proton or a neutron can be written as

$$\Psi_{n_\rho n_z \Lambda_z \Omega_z} = \psi_{n_\rho n_z}(\rho, z) \frac{[e^{i\Lambda_z \phi} \chi_{s_z}]^{\Omega_z}}{\sqrt{2\pi}}, \quad (1)$$

and the single-particle wave equation is

$$\left[-\frac{\hbar^2}{2m} \left\{ \frac{1}{\rho} \frac{\partial}{\partial \rho} \rho \frac{\partial}{\partial \rho} + \frac{\partial^2}{\partial z^2} - \frac{\Lambda_z^2}{\rho^2} \right\} + V(\rho, z) - \epsilon_{n_\rho n_z \Lambda_z \Omega_z} \right] \psi_{n_\rho n_z}(\rho, z) = 0, \quad (2)$$

where n_ρ and n_z are the quantum numbers associated with the oscillations in the ρ and z directions, Λ_z is the orbital angular momentum component along the z -direction, and $\Omega_z = \Lambda_z + s_z$. We are interested in the phenomenology of a ^{12}C nucleus with a toroidal density distribution in ^{12}C for which the oscillation energy in the ρ and z directions are substantially greater than the orbital energy associated with the Λ_z quantum number. In such a case, the latter can be treated as a perturbation. We are also interested in particle-hole excitations involving single-particle states with $n_\rho=0$ and $n_z=0$ whose labels will be omitted. Upon neglecting the small spin-orbit interaction for low-lying states with low orbital angular momenta, the single-particle energy of the lowest states are

$$\epsilon_{\Lambda_z \Omega_z} = \epsilon_{\rho z 0} + \frac{\hbar^2 \Lambda_z^2}{2mR^2}, \quad (3)$$

where $\epsilon_{\rho z 0}$ is the zero-point energy associated with oscillations in the $V(\rho, z)$ potential, and the effective major radius R is a measure of the matrix element

$$\frac{\hbar^2 \Lambda_z^2}{2mR^2} = \langle \psi_{n_\rho=0, n_z=0}(\rho, z) | \frac{\hbar^2 \Lambda_z^2}{2m\rho^2} | \psi_{n_\rho=0, n_z=0}(\rho, z) \rangle. \quad (4)$$

To get the lowest lying particle-hole excitation spectrum of the toroidal nucleus in question, we place the nucleons

in the lowest single-particle states in the toroidal potential, make the single-particle particle-hole excitations between different $|\Lambda_z \Omega_z\rangle$ states without exciting the oscillations in the ρ and z directions, and record their excitation energies and quantum numbers.

III. PARTICLE-HOLE EXCITATIONS OF A TOROIDAL NUCLEUS

With the single-particle state energies given by Eq. (3) for a toroidal nucleus, the density of single-particle states in the energy spacing is far from being uniform in a toroidal nucleus. The single-particle state energies depend only on the absolute value $\Lambda \equiv |\Lambda_z|$. They group together into toroidal “ Λ -shells”, with a large energy gap between one toroidal Λ -shell and the next, generating magic numbers $N=2(2\Lambda+1)$ in the light-mass region [66, 67]. As shown schematically in Fig. 1, the toroidal ground state of the ^{12}C nucleus with the closed toroidal shells is described by nucleons occupying the $\Lambda=0$ and $\Lambda=1$ toroidal shells, filling up the lowest single-particle states of $|0 \pm \frac{1}{2}\rangle$, $|1 \pm \frac{1}{2}\rangle$, $|1 \pm \frac{3}{2}\rangle$.

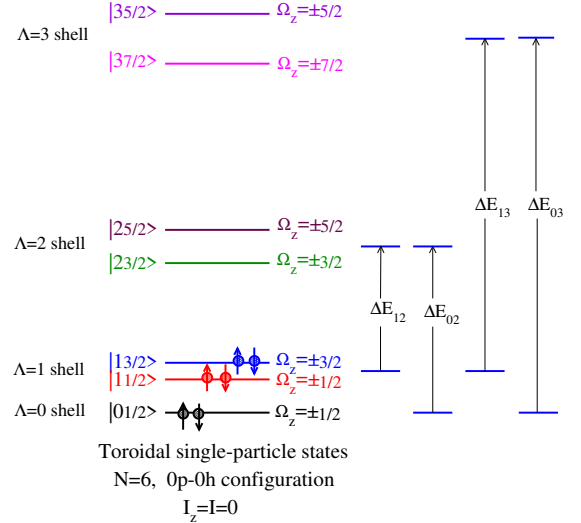


FIG. 1. (Color online.) Schematic toroidal single-particle energy level diagram for neutrons or protons, with the nucleons occupying the lowest $|\Lambda_z \Omega_z\rangle$ single-particle states for the ^{12}C nucleus in the toroidal configuration. The excitation energies $\Delta E_{\Lambda_i \Lambda_f}$ for various $(1p1h)_{\Lambda_i \Lambda_f}$ excitations from the Λ_i toroidal shell to the Λ_f toroidal shell are schematically indicated.

The doubly closed-shell nature of the ^{12}C nucleus in the toroidal configuration means that the energy gap between the occupied states in the $\Lambda=1$ shell and the unoccupied states in the $\Lambda=2$ shell is expected to be quite large, presumably much larger than the spin-orbit and residual interactions. Thus, the particle-hole excitations from one Λ -shell to another will yield the gross structure, while the spin-orbit and residual interactions will provide the fine structure of the spectrum. In the

present first survey we shall contend ourselves only with the gross structure by studying particle-hole excitations built on toroidal single-particle shells without spin-orbit and residual interactions. Refinement of the energy spectrum can be carried out in the projected shell model calculations using the toroidal states as basis states as in [81–84].

We can use the single-particle energies Eq. (3) to determine the gross structure of the particle-hole excitation of a double-closed shell toroidal nucleus by calculating the particle-hole excitation energy $E_I - E_0$ and its associated angular momentum component I_z . We call the angular momentum component I_z along the symmetry axis with $I_z = I$ the spin I (or I_z) of the toroidal state.

We construct the multiplet of (n particle)-(n hole) excitations by promoting n nucleons from the occupied Λ_i -shell to the empty Λ_f -shell. We label the multiplet as $(\text{nph})_{\Lambda_i\Lambda_f}^\pi$, where π , the parity of the multiplet, is equal to $(-1)^{\Lambda_f - \Lambda_i}$. In particular, the $(1\text{p}1\text{h})_{\Lambda_i\Lambda_f}^\pi$ multiplet of particle-hole excitations can be constructed by promoting a nucleon from an occupied initial state $|\Lambda_z\Omega_z\rangle_i$ in the Λ_i -shell to an unoccupied final state $|\Lambda_z\Omega_z\rangle_f$ in the Λ_f -shell. Such an $\{i \rightarrow f\}$ particle-hole excitation leads to a spin increment $\Delta_{if}I_z$ given by

$$\Delta_{if}I_z(|\Lambda_z\Omega_z\rangle_i \rightarrow |\Lambda_z\Omega_z\rangle_f) = \Omega_{zf} - \Omega_{zi}, \quad (5)$$

and from Eq. (3) an excitation energy increment $\Delta_{if}E_{\Lambda_i\Lambda_f}$ given by

$$\begin{aligned} \Delta_{if}E_{\Lambda_i\Lambda_f}(|\Lambda_z\Omega_z\rangle_i \rightarrow |\Lambda_z\Omega_z\rangle_f) &= \epsilon(|\Lambda_z\Omega_z\rangle_f) - \epsilon(|\Lambda_z\Omega_z\rangle_i) \\ &= \frac{\hbar^2}{2mR^2} (\Lambda_f^2 - \Lambda_i^2). \end{aligned} \quad (6)$$

Here the energy unit $\hbar^2/2mR^2$ appears so frequently in the excitation energy expressions that it deserves a symbol of its own. We call it ϵ_0 ,

$$\epsilon_0 = \frac{\hbar^2}{2mR^2}. \quad (7)$$

The spin I_z and excitation energy E_x of a state in the $(\text{nph})_{\Lambda_i\Lambda_f}^\pi$ multiplet, in the simplest approximation with the neglect of spin-orbit and residual interactions, are just additive sums of the spin and energy increments from independent $\{i \rightarrow f\}$ particle-hole excitations, subject to the Pauli exclusion principle,

$$I_z = \sum_{if} \Delta_{if}I_z(|\Lambda_z\Omega_z\rangle_i \rightarrow |\Lambda_z\Omega_z\rangle_f). \quad (8)$$

The parity π of the state is

$$\pi = \prod_{if} \{(-1)^{\Lambda_f - \Lambda_i}\}. \quad (9)$$

Because there are many different Ω_z states in a single-particle Λ -shell, there are many different spin increments in an $(\text{nph})_{\Lambda_i\Lambda_f}^\pi$ multiplet. Consequently there are many different I_z spins in the multiplet states of the toroidal nucleus. All these states with different spins

$I = I_z$ within the multiplet have the same parity π and are degenerate with the excitation energy

$$E_x = E_I - E_0 = \sum_{if} \Delta_{if}E_{\Lambda_i\Lambda_f}(|\Lambda_z\Omega_z\rangle_i \rightarrow |\Lambda_z\Omega_z\rangle_f), \quad (10)$$

where E_0 is the energy of the toroidal ground state relative to the ^{12}C ground state. The inclusion of spin-orbit and residual interactions in a more refined calculation will split the degeneracy of the different I_z states in the multiplet.

IV. SPECTRUM OF THE ^{12}C NUCLEUS IN THE TOROIDAL CONFIGURATION

A. $(1\text{p}1\text{h})_{\Lambda_i\Lambda_f}^\pi$ Toroidal States

As one can see from Fig. 1, different $(1\text{p}1\text{h})_{\Lambda_i\Lambda_f}^\pi$ multiplets of excited ^{12}C toroidal states arise by promoting nucleons from $\{[0(\pm 1/2)], [1(\pm 1/2)], [1(\pm 3/2)]\}$ toroidal states in the $\Lambda=0$ and 1 shells to occupy empty $\{[2(\pm 5/2)], [2(\pm 3/2)], [3(\pm 7/2)], [3(\pm 5/2)]\}$ toroidal states in the $\Lambda=2$ and 3 shells. The knowledge of the particle and hole state quantum numbers gives the spin and parity of the excitation, and the excitation energy can be determined from the single-particle energy (3) or the energy increment (6). In particular, for a member I_z^π with $I = I_z$ in the $(1\text{p}1\text{h})_{\Lambda_i\Lambda_f}^\pi$ multiplet, the energy E_I of the member relative to the toroidal ground state of energy E_0 is $E_I - E_0 = \Delta E_{\Lambda_i\Lambda_f}$. All members of a multiplet have the same excitation energy in the present idealized approximation with the neglect of the spin-orbit and residual interactions.

The (one particle)-(one hole) $\Delta E_{\Lambda_i\Lambda_f}$ for different shell-to-shell excitations are

$$\Delta E_{12} = \epsilon(\Lambda = 1) \rightarrow \epsilon(\Lambda = 2) = \frac{3\hbar^2}{2mR^2} = 3\epsilon_0, \quad (11a)$$

$$\Delta E_{02} = \epsilon(\Lambda = 0) \rightarrow \epsilon(\Lambda = 2) = \frac{4\hbar^2}{2mR^2} = 4\epsilon_0, \quad (11b)$$

$$\Delta E_{13} = \epsilon(\Lambda = 1) \rightarrow \epsilon(\Lambda = 3) = \frac{8\hbar^2}{2mR^2} = 8\epsilon_0, \quad (11c)$$

$$\Delta E_{03} = \epsilon(\Lambda = 0) \rightarrow \epsilon(\Lambda = 3) = \frac{9\hbar^2}{2mR^2} = 9\epsilon_0. \quad (11d)$$

These excitation energies depend only on a single-parameter, the major radius R , which can be determined by confronting the predicted theoretical spectrum with the experimental data in the next Section. For particle-hole excitations among the lowest states with $n_\rho = 0$ and $n_z = 0$, the above equations indicate that the excitation energies are independent of the shape of the underlying toroidal potential $V(\rho, z)$. The parity of a member I_z^π member of the $(1\text{p}1\text{h})_{\Lambda_i\Lambda_f}^\pi$ multiplet, is $\pi = (-1)^{\Lambda_f - \Lambda_i}$.

TABLE I. The $(1p1h)_{\Lambda_i\Lambda_f}^{\pi}$ excitations in toroidal ^{12}C where $[\Lambda_f\Omega_{zf}]$ represents a particle state and $[\Lambda_i\Omega_{zf}]^{-1}$ represents the hole state.

particle-hole excitation	particle-hole configuration	I_z^{π}	$\frac{E_I - E_0}{\epsilon_0}$
$(1p1h)_{12}^{-}$ $\Lambda=1$ shell $\rightarrow \Lambda=2$ shell	$[1(-3/2)]^{-1}[2(5/2)]$	4^{-}	3
	$[1(-1/2)]^{-1}[2(5/2)]$	3^{-}	
	$[1(1/2)]^{-1}[2(5/2)]$	2^{-}	
	$[1(3/2)]^{-1}[2(5/2)]$	1^{-}	
	$[1(-3/2)]^{-1}[2(3/2)]$	3^{-}	
	$[1(-1/2)]^{-1}[2(3/2)]$	2^{-}	
	$[1(1/2)]^{-1}[2(3/2)]$	1^{-}	
	$[1(3/2)]^{-1}[2(3/2)]$	0^{-}	
$(1p1h)_{02}^{+}$ $\Lambda=0$ shell $\rightarrow \Lambda=2$ shell	$[0(-1/2)]^{-1}[2(5/2)]$	3^{+}	4
	$[0(1/2)]^{-1}[2(5/2)]$	2^{+}	
	$[0(-1/2)]^{-1}[2(3/2)]$	2^{+}	
	$[0(1/2)]^{-1}[2(3/2)]$	1^{+}	
$(1p1h)_{13}^{+}$ $\Lambda=1$ shell $\rightarrow \Lambda=3$ shell	$[1(-3/2)]^{-1}[3(7/2)]$	5^{+}	8
	$[1(-1/2)]^{-1}[3(7/2)]$	4^{+}	
	$[1(1/2)]^{-1}[3(7/2)]$	3^{+}	
	$[1(3/2)]^{-1}[3(7/2)]$	2^{+}	
	$[1(-3/2)]^{-1}[3(5/2)]$	4^{+}	
	$[1(-1/2)]^{-1}[3(5/2)]$	3^{+}	
	$[1(1/2)]^{-1}[3(5/2)]$	2^{+}	
	$[1(3/2)]^{-1}[3(5/2)]$	1^{+}	
$(1p1h)_{03}^{-}$ $\Lambda=0$ shell $\rightarrow \Lambda=3$ shell	$[0(-1/2)]^{-1}[3(7/2)]$	4^{-}	9
	$[0(1/2)]^{-1}[3(7/2)]$	3^{-}	
	$[0(-1/2)]^{-1}[3(5/2)]$	3^{-}	
	$[0(1/2)]^{-1}[3(5/2)]$	2^{-}	

We show the spin quantum number I_z , parity π , and the excitation energy $E_I - E_0$ of different $(1p1h)_{\Lambda_i\Lambda_f}^{\pi}$ multiplets of excited toroidal states in Table I. We have kept the sign of Ω_z of the particle state positive. If we study the remaining case by reversing the sign of Ω_z of the particle state, we obtain the same set of states as in Table I, except that the signs of I_z is reversed if it is non-zero, and it has a different particle-hole combination if I_z is zero. Thus, each of the total set of states in Table I is doubly degenerate. The double degeneracy occurs repeatedly in all toroidal states, and we shall make its double degeneracy implicit and shall consider only non-negative values of I_z with double degeneracy in what follows, unless explicitly specified otherwise. Furthermore, it should be kept in mind that Table I is applicable to neutron as well as to proton $(1p1h)$ excitations.

Table I and Fig. 2 show that the $(1p1h)_{12}^{\pi}$ multiplet for the excitation of a nucleon from the $\Lambda=1$ shell to the $\Lambda=2$ shell consists of a set of eight doubly-degenerate states, $\{4^{-}, 2(3^{-}), 2(2^{-}), 2(1^{-}), 0^{-}\}$, lying at $E_x = E_I - E_0 = 3\epsilon_0$. The $(1p1h)_{02}^{+}$ multiplet for the excitation of a nucleon from the $\Lambda=0$ shell to the $\Lambda=2$ shell consists of a set of four states, $\{3^{+}, 2(2^{+}), 1^{+}\}$, lying at an excitation energy $E_x = 4\epsilon_0$. The $(1p1h)_{13}^{+}$ multiplet for the excitation of a nucleon from the $\Lambda=1$ shell to the $\Lambda=3$ shell consists of a set of eight states of $\{5^{+}, 2(4^{+}), 2(3^{+}), 2(2^{+}), 1^{+}\}$ lying at $E_x = 8\epsilon_0$. Finally, the $(1p1h)_{03}^{-}$ multiplet for the excitation of a nucleon

from the $\Lambda=0$ shell to the $\Lambda=3$ shell consists of a set of four doubly-degenerate states, $\{4^{-}, 2(3^{-}), 2^{-}\}$, lying at $E_x = 9\epsilon_0$. The spectrum of these states are shown in Fig. 2.

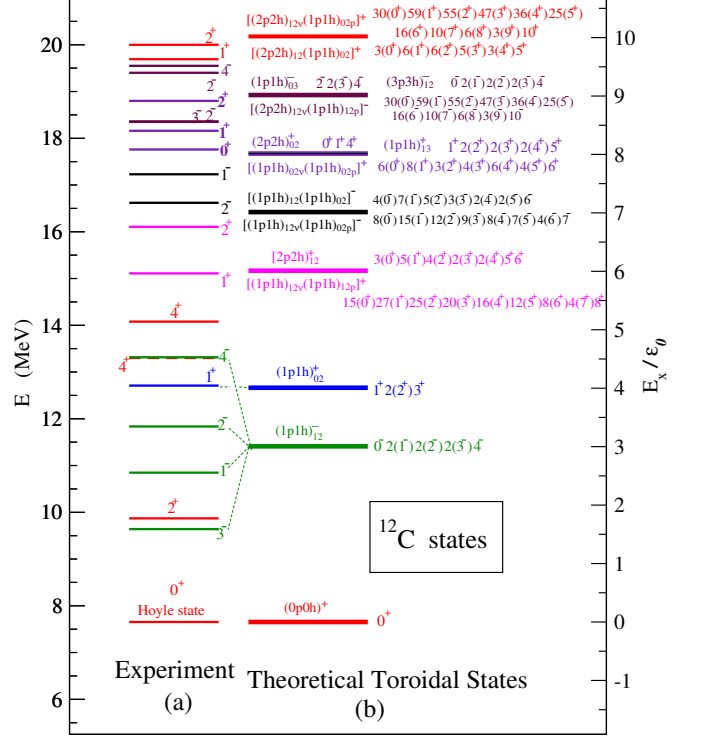


FIG. 2. (color online). (a) Experimental excitation energy E of ^{12}C excited states relative to the ^{12}C ground state [14], with the axis of the excitation energy E on the left. (b) The theoretical spectrum of the toroidal states in different multiplets, with the axis of the excitation energy $E_x = E - E_0$, relative to the energy E_0 of the toroidal ground state, given on the right. Comparison between the experimental and theoretical spectra is made by identifying the Hoyle state as the toroidal ground state and the lowest lying $3^{-}, 1^{-}, 2^{-}, 4^{-}$ as members of the toroidal $(1p1h)_{12}^{-}$ multiplet, leading to $\epsilon_0 = 1.25$ MeV (see text). The spins and parities of members of the multiplets are presented in the figure and given in Table VI.

The lowest lying toroidal states are the $(0p0h)^+$, $(1p1h)_{12}^{-}$, and $(1p1h)_{02}^{+}$ multiplets lying above the ground toroidal ^{12}C state. They should be prominently excited by stripping ($^3\text{He}, d$) reactions that add a proton to excite and combine with a ^{11}B nucleus to a toroidal configuration.

B. $(2p2h)_{12}^{+}$ at $E_x = 6\epsilon_0$ for exciting two identical nucleons from $\Lambda=1$ shell to $\Lambda=2$ shell

We consider next the $(2p2h)_{12}^{+}$ excitations of two identical particles (neutrons or protons) from the $\Lambda=1$ shell to the $\Lambda=2$ shell. Because of the Pauli exclusion principle, the two identical particle or holes cannot occupy the

same $|\Lambda_z, \Omega_z\rangle$ state. Consequently, to get the (2 particle)-(2 hole) excitations involving identical particles, it is simplest to combine the angular momentum components of the two particles and two holes separately first, under the restriction of the Pauli principle, before combining them together. For this purpose, we list all combinations of states of two holes in Table II and two particles in Table III, under the restriction of the Pauli principle.

TABLE II. Combination of two holes states in $|1(\pm 3/2)\rangle$ and $|1(\pm 1/2)\rangle$ states in the $\Lambda=1$ shell under the restriction of the Pauli principle

two hole configuration	I_z^π
$\{[1(3/2)][1(1/2)]\}^{-1}$	$[2^+]^{-1}$
$\{[1(3/2)][1(-1/2)]\}^{-1}$	$[1^+]^{-1}$
$\{[1(1/2)][1(-1/2)]\}^{-1}$	$[0^+]^{-1}$
$\{[1(-3/2)][1(3/2)]\}^{-1}$	$[0^+]^{-1}$
$\{[1(-3/2)][1(1/2)]\}^{-1}$	$[(-1)^+]^{-1}$
$\{[1(-3/2)][1(-1/2)]\}^{-1}$	$[(-2)^+]^{-1}$

TABLE III. Combination of two particles states in $|2 \pm 5/2\rangle$ and $|2 \pm 3/2\rangle$ orbitals in the $\Lambda=2$ shell under the restriction of the Pauli principle

two particle configuration	I_z^π
$\{[2(5/2)][2(3/2)]\}$	4^+
$\{[2(5/2)][2(-3/2)]\}$	1^+
$\{[2(3/2)][2(-3/2)]\}$	0^+
$\{[2(-5/2)][2(5/2)]\}$	0^+
$\{[2(-5/2)][2(3/2)]\}$	$(-1)^+$
$\{[2(-5/2)][2(-3/2)]\}$	$(-4)^+$

Now combine the two hole states with all two particle states, we get the angular momentum component I_z and parity π as listed in Table IV. As one observes in Table IV, the $(2p2h)_{12}^+$ multiplet consists of a set of 18 doubly-degenerate positive parity states, $\{6^+, 5^+, 2(4^+), 2(3^+), 4(2^+), 5(1^+), 3(0^+)\}$, lying at $E_x = 6\epsilon_0$ as shown in Fig. 2(b). It is applicable to a pair of neutrons or protons.

TABLE IV. The spin states of the $(2p2h)_{12}^+$ multiplet at $E_x=6\epsilon_0$ for the excitation of two identical nucleons from the $\Lambda=1$ shell to the $\Lambda=2$ shell

two holes	two particle configuration	I_z^π
$\{[1(3/2)][1(1/2)]\}^{-1}$	$\{[2(5/2)][2(3/2)]\}$	2^+
	$\{[2(5/2)][2(-3/2)]\}$	$(-1)^+$
	$\{[2(3/2)][2(-3/2)]\}$	$(-2)^+$
	$\{[2(-5/2)][2(5/2)]\}$	$(-2)^+$
	$\{[2(-5/2)][2(3/2)]\}$	$(-3)^+$
	$\{[2(-5/2)][2(-3/2)]\}$	$(-6)^+$
$\{[1(3/2)][1(-1/2)]\}^{-1}$	$\{[2(5/2)][2(3/2)]\}$	3^+
	$\{[2(5/2)][2(-3/2)]\}$	0^+
	$\{[2(3/2)][2(-3/2)]\}$	$(-1)^+$
	$\{[2(-5/2)][2(5/2)]\}$	$(-1)^+$
	$\{[2(-5/2)][2(3/2)]\}$	$(-2)^+$
	$\{[2(-5/2)][2(-3/2)]\}$	$(-5)^+$
$\{[1(1/2)][1(-1/2)]\}^{-1}$	$\{[2(5/2)][2(3/2)]\}$	4^+
	$\{[2(5/2)][2(-3/2)]\}$	1^+
	$\{[2(3/2)][2(-3/2)]\}$	0^+
	$\{[2(-5/2)][2(5/2)]\}$	0^+
	$\{[2(-5/2)][2(3/2)]\}$	$(-1)^+$
	$\{[2(-5/2)][2(-3/2)]\}$	$(-4)^+$
$\{[1(-3/2)][1(3/2)]\}^{-1}$	$\{[2(5/2)][2(3/2)]\}$	4^+
	$\{[2(5/2)][2(-3/2)]\}$	1^+
	$\{[2(3/2)][2(-3/2)]\}$	0^+
	$\{[2(-5/2)][2(5/2)]\}$	0^+
	$\{[2(-5/2)][2(3/2)]\}$	$(-1)^+$
	$\{[2(-5/2)][2(-3/2)]\}$	$(-4)^+$
$\{[1(-3/2)][1(1/2)]\}^{-1}$	$\{[2(5/2)][2(3/2)]\}$	5^+
	$\{[2(5/2)][2(-3/2)]\}$	2^+
	$\{[2(3/2)][2(-3/2)]\}$	1^+
	$\{[2(-5/2)][2(5/2)]\}$	1^+
	$\{[2(-5/2)][2(3/2)]\}$	0^+
	$\{[2(-5/2)][2(-3/2)]\}$	$(-3)^+$
$\{[1(-3/2)][1(-1/2)]\}^{-1}$	$\{[2(5/2)][2(3/2)]\}$	6^+
	$\{[2(5/2)][2(-3/2)]\}$	3^+
	$\{[2(3/2)][2(-3/2)]\}$	2^+
	$\{[2(-5/2)][2(5/2)]\}$	2^+
	$\{[2(-5/2)][2(3/2)]\}$	1^+
	$\{[2(-5/2)][2(-3/2)]\}$	$(-2)^+$

C. $[(1p1h)_{12\nu}(1p1h)_{12p}]^+$ toroidal multiplet involving one neutron and one proton

In the last subsection, we have considered the $(2p2h)$ excitations involving two identical nucleons. The case of the $(2p2h)$ excitations involving two different types of nucleons from the $\Lambda = 1$ shell to the $\Lambda = 2$ shell differ from the previous case, because the pairs of particles or holes do not need to be restricted by the Pauli principle. We can consider such $(2p2h)$ excitations by combining a $(1p1h)$ neutron excitation with an independent $(1p1h)$ proton excitation. Such a $[(1p1h)_{12\nu}(1p1h)_{12p}]^\pi$ multiplet has the excitation energy $E_x = 2\Delta E_{12} = 6\epsilon_0$ and positive parity. In the notation for the multiplet, we have used the subscript ν for neutrons and p for protons. Their spin quantum numbers I_z and parities are given in

Table V.

TABLE V. The spin states of the $[(1p1h)_{12\nu}(1p1h)_{12p}]^+$ multiplet at $E_x=6\epsilon_0$ involving different types of nucleons

(1p1h) _{12ν} State	(1p1h) _{12p} State							
	4 ⁻	3 ⁻	2 ⁻	1 ⁻	3 ⁻	2 ⁻	1 ⁻	0 ⁻
4 ⁻	8 ⁺	7 ⁺	6 ⁺	5 ⁺	7 ⁺	6 ⁺	5 ⁺	4 ⁺
3 ⁻	7 ⁺	6 ⁺	5 ⁺	4 ⁺	6 ⁺	5 ⁺	4 ⁺	3 ⁺
2 ⁻	6 ⁺	5 ⁺	4 ⁺	3 ⁺	5 ⁺	4 ⁺	3 ⁺	2 ⁺
1 ⁻	5 ⁺	4 ⁺	3 ⁺	2 ⁺	4 ⁺	3 ⁺	2 ⁺	1 ⁺
3 ⁻	7 ⁺	6 ⁺	5 ⁺	4 ⁺	6 ⁺	5 ⁺	4 ⁺	3 ⁺
2 ⁻	6 ⁺	5 ⁺	4 ⁺	3 ⁺	5 ⁺	4 ⁺	3 ⁺	2 ⁺
1 ⁻	5 ⁺	4 ⁺	3 ⁺	2 ⁺	4 ⁺	3 ⁺	2 ⁺	1 ⁺
0 ⁻	4 ⁺	3 ⁺	2 ⁺	1 ⁺	3 ⁺	2 ⁺	1 ⁺	0 ⁺
(-4) ⁻	0 ⁺	(-1) ⁺	(-2) ⁺	(-3) ⁺	(-1) ⁺	(-2) ⁺	(-3) ⁺	(-4) ⁺
(-3) ⁻	1 ⁺	0 ⁺	(-1) ⁺	(-2) ⁺	0 ⁺	(-1) ⁺	(-2) ⁺	(-3) ⁺
(-2) ⁻	2 ⁺	1 ⁺	0 ⁺	(-1) ⁺	1 ⁺	0 ⁺	(-1) ⁺	(-2) ⁺
(-1) ⁻	3 ⁺	2 ⁺	1 ⁺	0 ⁺	2 ⁺	1 ⁺	0 ⁺	(-1) ⁺
(-3) ⁻	1 ⁺	0 ⁺	(-1) ⁺	(-2) ⁺	0 ⁺	(-1) ⁺	(-2) ⁺	(-3) ⁺
(-2) ⁻	2 ⁺	1 ⁺	0 ⁺	(-1) ⁺	(-2) ⁺	0 ⁺	(-1) ⁺	(-2) ⁺
(-1) ⁻	3 ⁺	2 ⁺	1 ⁺	0 ⁺	2 ⁺	1 ⁺	0 ⁺	(-1) ⁺
0 ⁻	4 ⁺	3 ⁺	2 ⁺	1 ⁺	3 ⁺	2 ⁺	1 ⁺	0 ⁺

There are altogether $\{8^+, 4(7^+), 8(6^+), 12(5^+), 15(4^+), 16(3^+), 16(2^+), 15(1^+), 15(0^+), 1(-4)^+, 4(-3)^+, 9(-2)^+, 12(-1)^+\}$ for a total of 128 states. If we reverse the sign of the $(1p1h)_{12p}$ state, we get the same set of states but with the signs of I_z is reversed if it is non-zero, and it has a different particle-hole combination if I_z is zero. The $(I_z)^+$ and the $(-I_z)^+$ states in these two sets can be grouped together. In this new grouping, the combined set contains 128 doubly-degenerate states of the set $\{8^+, 4(7^+), 8(6^+), 12(5^+), 16(4^+), 20(3^+), 25(2^+), 27(1^+), 15(0^+)\}$ at the excitation energy $E_x=2\Delta E_{12}=6\epsilon_0$.

We have thus obtained the spectrum of the lowest-lying multiplets of states. The spectrum of the higher states can be obtained in a similar way. We can summarize the theoretical energy spectrum of the toroidal ^{12}C nucleus in Table VI and in Fig. 2.

TABLE VI. The theoretical spectrum of ^{12}C in a toroidal configuration. Here, $E_x=E_I-E_0$, E_I is the energy of a state in the multiplet, E_0 is the toroidal ground state energy, $\epsilon_0=1.25$ MeV by matching with the experimental spectrum, and N is the number of doubly-degenerate states in the multiplet.

Toroidal Ground State & Toroidal Multiplets	$\frac{E_x}{\epsilon_0}$	E_I (MeV)	$I_z=I$ states	N
$[(0p0h)]^+$	0	7.654	0^+	1
$[(1p1h)_{12}]^-$	3	11.41	$0^-, 2(1^-), 2(2^-), 2(3^-), 4^-$	8
$[(1p1h)_{02}]^+$	4	12.66	$1^+, 2(2^+), 3^+$	4
$[(2p2h)_{12}]^+$	6	15.16	$3(0^+), 5(1^+), 4(2^+), 2(3^+), 2(4^+), 5^+, 6^+$	18
$[(1p1h)_{12\nu}(1p1h)_{12p}]^+$	6	15.16	$15(0^+), 27(1^+), 25(2^+), 20(3^+), 16(4^+), 12(5^+), 8(6^+), 4(7^+), 8^+$	128
$[(1p1h)_{12}(1p1h)_{02}]^-$	7	16.42	$4(0^-), 7(1^-), 5(2^-), 3(3^-), 2(4^-), 2(5^-), 6^-$	24
$[(1p1h)_{12\nu}(1p1h)_{02p}]^-$	7	16.42	$8(0^-), 15(1^-), 12(2^-), 9(3^-), 8(4^-), 7(5^-), 4(6^-), 7^-$	64
$[(1p1h)_{13}]^+$	8	17.67	$1^+, 2(2^+), 2(3^+), 2(4^+), 5^+$	8
$[(2p2h)_{02}]^+$	8	17.67	$0^+, 1^+, 4^+$	3
$[(1p1h)_{02\nu}(1p1h)_{02p}]^+$	8	17.67	$6(0^+), 8(1^+), 3(2^+), 4(3^+), 6(4^+), 4(5^+), 6^+$	32
$[(1p1h)_{03}]^-$	9	18.92	$2^-, 2(3^-), 4^-$	8
$[(3p3h)_{12}]^-$	9	18.92	$0^-, 2(1^-), 2(2^-), 2(3^-), 4^-$	8
$[(2p2h)_{12\nu}(1p1h)_{12p}]^-$	9	18.92	$30(0^-), 59(1^-), 55(2^-), 47(3^-), 36(4^-), 25(5^-), 16(6^-), 10(7^-), 6(8^-), 3(9^-), 10^-$	288
$[(2p2h)_{12p}(1p1h)_{12\nu}]^-$	9	18.92	(same as above)	288
$[(2p2h)_{12}(1p1h)_{02}]^+$	10	20.15	$3(0^+), 6(1^+), 6(2^+), 5(3^+), 3(4^+), 5^+$	24
$[(2p2h)_{12p}(1p1h)_{02\nu}]^+$	10	20.15	$15(0^+), 30(1^+), 29(2^+), 25(3^+), 18(4^+), 11(5^+), 7(6^+), 5(7^+), 3(8^+), 9^+$	144
$[(2p2h)_{12\nu}(1p1h)_{02p}]^+$	10	20.15	(same as above)	144
$[(2p2h)_{02}(1p1h)_{12}]^-$	11	21.40	$4^-, 2(3^-), 2(2^-), 2(1^-), 0^-$	8
$[(4p4h)_{12}]^+$	12	22.65	0^+	1
$[(2p2h)_{12\nu}(2p2h)_{12p}]^+$	12	22.65	$69(0^+), 130(1^+), 117(2^+), 96(3^+), 78(4^+), 58(5^+), 42(6^+), 26(7^+), 16(8^+), 8(9^+), 5(10^+), 2(11^+), 12^+$	648
$[(3p3h)_{12}(1p1h)_{02}]^-$	13	23.90	$0^-, 2(1^-), 2^-$	4
$[(3p3h)_{12\nu}(1p1h)_{02p}]^-$	13	23.90	$8(0^-), 15(1^-), 12(2^-), 9(3^-), 8(4^-), 7(5^-), 4(6^-), 7^-$	64
$[(3p3h)_{12p}(1p1h)_{02\nu}]^-$	13	23.90	(same as above)	64
$[(2p2h)_{12}(2p2h)_{02}]^+$	14	25.15	$0^+, 1^+, 2^+$	3
$[(2p2h)_{12\nu}(2p2h)_{02p}]^+$	14	25.15	$13(0^+), 23(1^+), 20(2^+), 15(3^+), 13(4^+), 10(5^+), 7(6^+), 3(7^+), 2(8^+), 9^+, 10^+$	108

For simplicity, the single-particle energies in Eq. (3) have been simplified to depend only on Λ_z^2/R^2 . Such a representation may be adequate for the lowest few toroidal shells. However, in a more realistic case, the single-particle potential should follow the toroidal density and should be a diffused potential with a finite depth. The higher toroidal shells are expected to be unbound.

As a consequence, there will be a termination of the (nph) toroidal excitations, indicated by the absence of bound toroidal particle-hole excitations at high energies and a rapid decrease of the density of toroidal particle-hole excitation states. It will be of interest to search for the excitation energy maximum in ^{12}C at which the toroidal particle lie in the continuum and there will be no more bound toroidal particle-hole excitations.

V. COMPARISON OF TOROIDAL SIGNATURE WITH EXPERIMENTAL ^{12}C SPECTRUM

In the last few sections, we show that the ^{12}C nucleus in a toroidal configuration possesses a distinct spectrum of with well defined spins, parities, and excitation energies. They arise from particle-hole excitations from a toroidal Λ_i -shell to another toroidal Λ_f -shell and represent the signature of the ^{12}C nucleus in the toroidal configuration. Using such a signature, we explore whether there may be toroidal states in ^{12}C build on the 0^+ Hoyle state at 7.654 MeV as the head of the toroidal band.

In our exploratory survey, we expect that the toroidal states of ^{12}C and the low-lying toroidal multiplets will show up as ^{12}C resonances among states that have a large probability to breakup into 3 alpha particles. We envisage that for a system that breaks into three alpha particles, an emitted alpha particle will be in contact with a Be nucleus at the moment of scission. The Be nucleus will likely be in the form of a two-alpha cluster. A rod configuration with a three-alpha cluster lies at around 16.5 MeV [62]. The configuration of the ^{12}C system that decays into three alpha particles at excitation energies below the onset of the rod configuration at about 16.5 MeV is likely to consist of a triangular cluster of alpha particles in various degrees of contact. Such a triangular clusters of three alpha particles has a probability amplitude overlap with the toroidal configuration and can originate from the evolution of a toroidal configuration under sausage deformation of order $\lambda=3$. Accordingly, we search for good candidate toroidal states in $^{10}\text{B}(^3\text{He},p)^{12}\text{C}^* \rightarrow 3\alpha$ and $^{11}\text{B}(^3\text{He},d)^{12}\text{C}^* \rightarrow 3\alpha$ reactions [15–17] as shown in Figs. 3, 4, and 5. We shall discuss the results of our search in the following subsections.

A. Comparison of $^{11}\text{B}(^3\text{He},d)^{12}\text{C}^* \rightarrow 3\alpha$ Spectrum with Toroidal $(1p1h)_{12}^-$ and $(1p1h)_{02}^+$ Multiplets

In the experiments of Kirsebom *et al.* [15, 16], excited intermediate $^{12}\text{C}^*$ states were produced by the bombardment of the ^3He projectile at 8.5 MeV onto a ^{11}B target by the $^3\text{He} + ^{11}\text{B} \rightarrow d + ^{12}\text{C}^*$ reaction, with the subsequent breakup of the $^{12}\text{C}^*$ intermediate state into three alpha particles, $^{12}\text{C}^* \rightarrow 3\alpha$. The complete kinematic data of the final deuterium d and the 3 alpha particles have been recorded with detectors of fine resolutions and segmentation to allow the determination of (i) the en-

ergy of the intermediate $^{12}\text{C}^*$ state, (ii) the history of its subsequent decay, and (iii) the energy distribution Dalitz plot of the 3 alpha particles. From these pieces of information, the spins and parities of the prominent ^{12}C resonances can be inferred. The complete kinematic data allow the removal of most of the random coincidences and decay channels that do not involve the production of intermediate excited states of $^{12}\text{C}^*$. The measurement is essentially free of background [85]. The spectrum as shown in Figs. 3(a) and 4(a) from Kirsebom *et al.* [15, 16] can be considered to be the spectrum for the produced intermediate excited $^{12}\text{C}^*$ states, which include both the identified ^{12}C resonances as well as unresolved and unidentified excited $^{12}\text{C}^*$ states, as we shall discuss below.

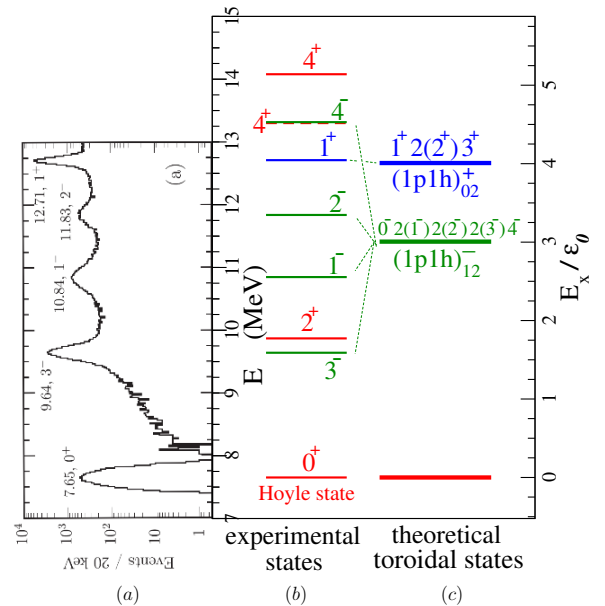


FIG. 3. (color online). (a) Experimental excitation function for the reaction $^{11}\text{B}(^3\text{He},d)^{12}\text{C}^* \rightarrow 3\alpha$ in logarithmic scale as a function of the $^{12}\text{C}^*$ excitation energy E in the range of $7 \leq E \leq 13$ MeV obtained by Kirsebom *et al.* [15], with the axis of the excitation energy on the left. (b) Experimental level scheme from the compilation of [14]. (c) Theoretical level scheme of toroidal states with the axis of $E_x = (E - E_0)/\epsilon_0$ on the right. Subsequent matching between theoretical and experimental excitation energies leads to $\epsilon_0=1.25$ MeV.

It is instructive to review how (i) the $^{11}\text{B}(^3\text{He},d)^{12}\text{C}^*$ reaction mechanism, (ii) the selection of the $^{12}\text{C}^* \rightarrow 3\alpha$ final states, and (iii) the knowledge of the toroidal nucleus structure information help guide us in the search for toroidal ^{12}C particle-hole excitation states. The $(^3\text{He},d)$ process of [15, 16] strips a proton from the incident projectile nucleus, ^3He , turns it into a deuterium, and deposits the stripped proton onto the target ^{11}B nucleus, which has 5 protons and 6 neutrons. With this addition of the stripped proton, the system with 6 protons and 6 neutrons completes a doubly-closed shell for a toroidal shape. By the selection of the breakup into three alpha particles, we judiciously search for the en-

ergy location for the ^{12}C toroidal state for processes in which the stripped proton can excite and polarize the nucleons in the ^{11}B system to re-configure themselves into a doubly closed shell toroidal nucleus with only a single unoccupied state in the proton $\Lambda=1$ shell, and the stripped proton can then fill up the unoccupied proton single-particle state to lead to the (0p0h) toroidal ^{12}C ground state.

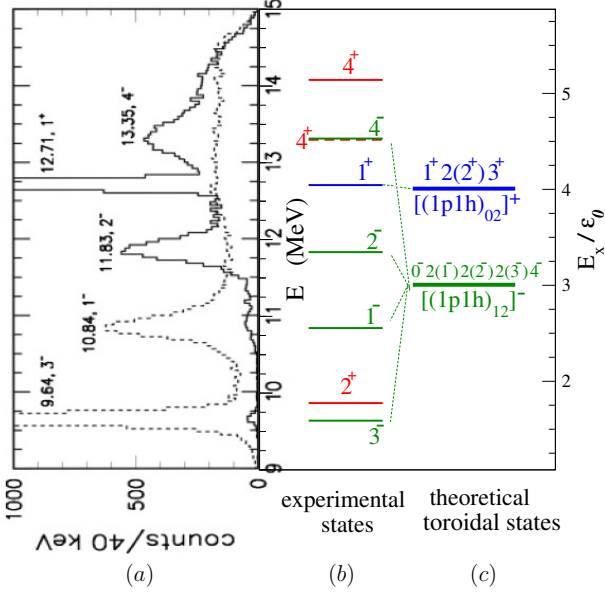


FIG. 4. (color online). Experimental excitation function for the reaction $^{11}\text{B}(^3\text{He},d)^{12}\text{C}^* \rightarrow 3\alpha$ in linear scale as a function of the $^{12}\text{C}^*$ excitation energy E in the range of $9 \leq E \leq 15$ MeV obtained by Kirsebom *et al.* [15], with the axis of the excitation energy on the left. (b) Experimental level scheme from the compilation of [14]. (c) Theoretical toroidal states with the axis of $E_x/\epsilon_0 = (E - E_0)/\epsilon_0$ on the right.

With the selection of breaking up into 3 alpha particles, we can look for events at another higher energy for the toroidal $(1p1h)_{12}^-$ ^{12}C state, in which the stripped proton excites the nucleons in the ^{11}B system to re-configure themselves into a toroidal configuration with a hole in the $\Lambda=1$ shell, while the stripped proton goes on to an unoccupied proton state in the higher unoccupied $\Lambda=2$ shell, leading to the $(1p1h)_{12}^-$ state of toroidal ^{12}C . We expect that at the appropriate energies, the $^{11}\text{B}(^3\text{He},d)^{12}\text{C}^* \rightarrow 3\alpha$ reaction should favorably populate (0p0h) and $(1p1h)_{12}^-$ states of the toroidal ^{12}C nucleus. In a similar manner, the $(1p1h)_{02}^+$ multiplets of $\{1^+, 2(2^+), 3^+\}$ in Table VI should be likewise favorably excited in the $^{11}\text{B}(^3\text{He},d)^{12}\text{C}^* \rightarrow 3\alpha$ reaction.

Figure 3(a) gives the experimental excitation function for the $^{11}\text{B}(^3\text{He},d)^{12}\text{C}^* \rightarrow 3\alpha$ reaction in the range $7 \leq E \leq 13$ MeV in logarithmic scale, and Fig. 4(a) shows the same excitation function in the range $9 \leq E \leq 15$ MeV in linear scale. Figs. 3(b) and 4(b) show the energy levels from the experimentally identified ^{12}C excited states from the compilation of [14]. The excitation energy E

relative to the energy of ^{12}C ground state is given on the left axis.

The experimental excitation functions in Figs. 3(a) and 4(a) indicate that the 0^+ Hoyle state at $E=7.654$ MeV is prominently excited, as are the 3^- state at 9.654 MeV, the 1^- state at 10.847 MeV, the 2^- state at 11.837 MeV, the 4^- state at 13.314 MeV, and the 1^+ state at 12.71 MeV. By comparing the experimental and the theoretical spectrum in Figs. 3(c) and 4(c), we find that the lowest theoretical multiplet in toroidal ^{12}C contains states with spins and parities that coincide with those of the experimental states. It is therefore reasonable to identify the 0^+ Hoyle state at 7.654 MeV to be the (0p0h) ground state of the toroidal configuration and the set of lowest $\{3^-(9.654 \text{ MeV}), 1^-(10.847 \text{ MeV}), 2^-(11.837 \text{ MeV}), 4^-(13.314 \text{ MeV})\}$ states to be members of the $(1p1h)_{12}^-$ multiplet. Following such an identification, we set the average excitation energy of the four states $\{3^-, 1^-, 2^-, 4^-\}$ at 11.41 MeV to be the excitation energy of the $(1p1h)_{12}^-$ multiplet. Such a matching leads to the theoretical energy scale,

$$\epsilon_0 = 1.25 \text{ MeV}. \quad (12)$$

By the definition of ϵ_0 as $\hbar^2/2mR^2$, we obtain the corresponding effective major radius,

$$R = 4.06 \text{ fm}. \quad (13)$$

The root-mean-squared radius r_{rms} of the Hoyle state as determined in previous 3α cluster theoretical models: $r_{\text{rms}}=3.56$ fm from the resonating group method in Ref. [33], $r_{\text{rms}}=3.40$ fm from the generator coordinate method in Ref. [30], $r_{\text{rms}}=3.83$ fm from the generator coordinate method in Ref. [35], and $r_{\text{rms}}=3.82$ fm from the three-body quantum dynamics in Ref. [23]. The value of R extracted from the (one-particle one-hole) spectrum here is slightly higher than the theoretical r_{rms} determined by cluster models calculations for the Hoyle state. Such a difference may arise partially from the fact that the particle-hole excitation involves the excitation to the unoccupied $\Lambda = 2$ single-particle orbital which has naturally a greater radius compared to the $\Lambda = 0$ and $\Lambda = 1$ occupied orbitals in the Hoyle state.

The knowledge of ϵ_0 allows the determination of the theoretical toroidal spectrum of ^{12}C as tabulated in Table VI and shown in Figs. 2-5. In particular, we find that the 1^+ state at $E_z=12.71$ MeV approximately matches the 1^+ state in the multiplet of $(1p1h)_{02}^+$.

We note in Figs. 3 and 4 that there are also a 2^+ state at 9.87 MeV, a 4^+ state at 13.3 MeV [86] and another 4^+ state at 14.079 MeV [14]. These states are collective rotational states that are not excited significantly by the stripping $^{11}\text{B}(^3\text{He},d)^{12}\text{C}^* \rightarrow 3\alpha$ reaction. The analysis of the interacting alpha particle model [87] and the algebraic cluster model [40, 41] found that the sequence of the 0_1^+ (ground state), 2_1^+ (4.33 MeV), and 4_2^+ (14.079 MeV) form the rotational states of the ground band, whereas the sequence of the Hoyle state 0_2^+ (7.654 MeV), 2_2^+ (9.870 MeV), and (4_1^+) (13.3 MeV) state [86] form a

rotational band with a different moment of inertia. With the identification of these rotational bands built on the Hoyle state and the ground state, a consistent description of the properties of all lowest eleven identified states of the ^{12}C nucleus emerges. Namely, in addition to the rotational $0^+, 2^+, 4^+$ bands of the ground state and the Hoyle state, the other low-lying states can be attributed simply to one-particle one-hole toroidal multiplet excitations from a spatially extended Hoyle state in the toroidal configuration.

B. Excitation Strength within the $(1p1h)_{12}^-$ Multiplet

The excitation function of the stripping reaction $^{11}\text{B}(^3\text{He},d)^{12}\text{C}^*$ leading to toroidal $(1p1h)_{12}^-$ particle-hole states in $^{12}\text{C}^*$ depends on the degree of occupation of the $\Lambda=1$ shell and the degree of emptiness of the unoccupied $\Lambda=2$ shell, which are the same for all members of the shell-to-shell particle-hole multiplet. Consequently, all members of the $(1p1h)_{12}^-$ multiplet should be approximately equally produced. An examination of the widths and the heights of the identified lowest $\{1^-, 2^-, 4^-\}$ states above the underlying unresolved states indicate that these three are approximately equally populated, supporting their identification as members of the $(1p1h)_{12}^-$ multiplet.

We note in passing that the experimental strength for the excitation of the $(0p0h)$ Hoyle state in Figure 3 is smaller than the strength for the excitation of the $(1p1h)$ states in the $^{11}\text{B}(^3\text{He},d)^{12}\text{C}^*$ reaction. In stripping a proton from the incident ^3He nucleus and depositing the proton onto the ^{11}B nucleus, the reaction of $^{11}\text{B}(^3\text{He},d)^{12}\text{C}^*$ is peripheral in nature. The dominant contribution to the reduced DWBA cross section depends on the tail of the radial single-particle bound-state wave functions of the deposited single-particle state inside the nucleus. The $(0p0h)$ excitation deposits a proton to the deeper $\Lambda = 1$ shell single-particle state whereas the $(1p1h)_{12}^-$ excitation deposit the proton to the higher $\Lambda = 2$ shell single-particle states with a greater magnitude of the wave function in the peripheral region of the nucleus. Therefore, the excitation strengths for the $(1p1h)_{12}^-$ ($3^-, 1^-, 2^-, 4^-$) multiplet is higher than that for the $(0p0h)$ 0^+ Hoyle state.

C. Number of Toroidal States in Multiplets and the Presence of Underlying Broad Structure

Our comparison with identified resonances reveals that there appear to be many more theoretical states than the number of experimentally identified states. On the other hand, the excitation function in Fig. 3(a) in the measurement of [15] possesses strengths away from the cleanly identified peaks. The measurement of [15] is free of background [85] because the complete kinemat-

ics satisfying the conservation of energy and momentum allow the identification all participating initial and final particles, and noise production of the $3\alpha+d$ assembly will not satisfy the energy and momentum conservation. Therefore, the presence of these extra excitation strength in Fig. 3(a) obtained in [15] indicates that additional overlapping resonances of ^{12}C have been produced in the $^{11}\text{B}(^3\text{He},d)^{12}\text{C}^* \rightarrow 3\alpha$ measurement. They constitute non-vanishing strengths in the Dalitz plot and represent broad and unidentified excited states of ^{12}C . They are likely the remaining members of the toroidal multiplets that are also produced. If they indeed are, then their number should match the remaining number of unidentified states. We can make a rough estimate of the remaining number of unidentified states as follows. Each state of the multiplet is expected to be produced in approximately an equal single-particle “particle-hole” strength in the stripping $^{11}\text{B}(^3\text{He},d)^{12}\text{C}^* \rightarrow 3\alpha$ reaction. The excitation function strengths of the resolved resonances in the range can be used as a yard stick to estimate the number of the remaining produced un-identified $^{12}\text{C}^*$ resonances in the underlying broad structure in Fig. 4(a).

In the data of Fig. 4(a), the $1^-(10.847 \text{ MeV})$, $2^-(11.837 \text{ MeV})$, and $4^-(13.314 \text{ MeV})$ resonances are members of the $(1p1h)_{12}^-$ multiplet arising from single-particle excitations populating a one-particle-one-hole state in the $\Lambda=2$ shell.

The strength of each the $1^-(10.847 \text{ MeV})$, $2^-(11.837 \text{ MeV})$, and $4^-(13.314 \text{ MeV})$ resonances as suggested members of the $(1p1h)_{12}^-$ multiple defines roughly a single-particle “particle-hole” unit, with approximately the same area for each of the three peaks, and each particle-hole unit leads to the production of one $^{12}\text{C}^*$ particle-hole state. On that basis of using that (average) area as a yardstick, we find that in the energy range of Fig. 4(a) up to the instrumental cut-off excitation energy of $\sim 14.5 \text{ MeV}$, there are approximately 3 to 5 units of particle-hole strength for natural parity states and 2 to 4 units for the un-natural parity states in the underlying overlapping resonances, with a considerable degrees of uncertainty in these numbers due to the uncertainty in separating out the resolved peaks from the underlying broad structure. The numbers of remaining un-identified members in the multiplet fall within the range of numbers of particle-hole states estimated to be present in the underlying broad structure in Fig. 4(a). By this comparison, it appears that the total number of identified and unidentified resonances produced in the $^{11}\text{B}(^3\text{He},d)^{12}\text{C}^* \rightarrow 3\alpha$ reaction matches approximately the total number of particle-hole states of the $(1p1h)_{12}^-$ and $(1p1h)_{02}^+$ multiplets.

D. The Excitation Function in $^{10}\text{B}(^3\text{He},p)^{12}\text{C}^* \rightarrow 3\alpha$ and the Density of Toroidal States at High Energies

In another experiment, Alcorta *et al.* [17] used the ^3He projectile to collide with a ^{10}B target nucleus to study the excited states of ^{12}C by the $^{10}\text{B}(^3\text{He},p)^{12}\text{C}^* \rightarrow 3\alpha$ reaction at a beam energy of 4.9 MeV. The complete kinematics of all four final particles were collected using detectors of fine resolution and segmentation. Again, the full knowledge of the complete kinematics facilitate the assignment of spins and parities. Contributions from direct reactions leading to the production of intermediate states other than $^{12}\text{C}^*$ have been eliminated as much as possible so that the excitation function of the 3α spectrum can also be considered to be essentially free of background, pending future removal of the small $^3\text{He} + ^{10}\text{B} \rightarrow ^8\text{Be} + ^5\text{Li} \rightarrow ^8\text{Be} + p + \alpha$ and $^3\text{He} + ^{10}\text{B} \rightarrow \alpha + ^9\text{B} \rightarrow \alpha + \alpha + ^5\text{Li}$ contributions [85].

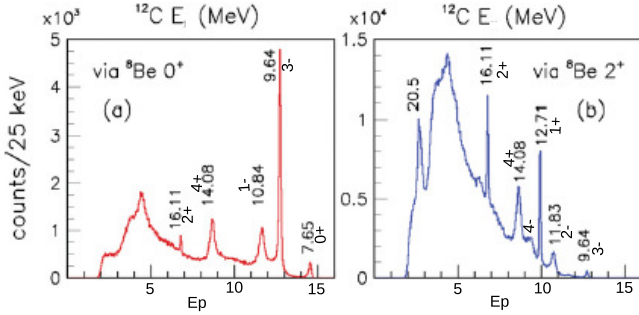


FIG. 5. (color online). Experimental excitation functions of the reaction $^{10}\text{B}(^3\text{He},p)^{12}\text{C}^* \rightarrow 3\alpha$ as a function of the proton energy E_p from Alcorta *et al.* [17]. The excitation energies E_x , spins, and parities of identified resonances of the excited $^{12}\text{C}^*$ states are indicated. Please note the different count scales on the y -axes in Figs. (a) and (b). The decay of the excited $^{12}\text{C}^*$ state goes through the 0^+ state of ^8Be in (a) and through the 2^+ state of ^8Be in (b).

The $(^3\text{He},p)$ reaction strips a neutron and a proton from the ^3He projectile and deposits the two nucleons onto the ^{10}B target. It is expected to populate favorably the $(0p0h)$, $(1p1h)$, and $(2p2h)$ toroidal excitations of $^{12}\text{C}^*$ at different excitation energies. Experiment data of the $^{10}\text{B}(^3\text{He},p)^{12}\text{C}^* \rightarrow 3\alpha$ reaction [17] in Fig. 5 in the three alpha breakup indicate that the Hoyle state, the lowest $\{1^-, 2^-, 3^-, 4^-\}$ and 1^+ states are prominently produced.

The additional possibility of the $(2p2h)$ excitations with the $^{10}\text{B}(^3\text{He},p)^{12}\text{C}^* \rightarrow 3\alpha$ reaction leads to an enhanced excitation function at higher excitation energies. It is interesting to note that the experimental $4^+(14.08 \text{ MeV})$ state and the $2^+(16.11 \text{ MeV})$ falls in the vicinity of the theoretical $(2p2h)_{12}^+$ multiplet whose members include a 2^+ and a 4^+ state. Whether these two states can be identified as two members of the $(2p2h)_{12}^+$ multiplet

will require further theoretical and experimental investigations. In Fig. 5 the produced resolved states appear as sharp peaks on top of an underlying broad structure. If we consider the sharp peaks as arising from a $2p2h$ excitation and we employ the earlier method using the areas of the excitation function covered by known resonances as a “two-particle-two-hole” ($2p2h$) yard stick to estimate the number of $(2p2h)$ states involved in the underlying broad structure, we would come up with the result that the number of similar $(2p2h)$ states comprising the underlying broad structure in Fig. 5 is an order of magnitude greater than number of resolved and identified resonances. Thus in addition to the few resolved and identified states that have been mentioned as possible members of the toroidal $(2p2h)$ multiplets, the underlying structure represents also a large number of possible produced members of the toroidal multiplets in the $^{10}\text{B}(^3\text{He},p)^{12}\text{C}^* \rightarrow 3\alpha$ reaction of Ref. [17].

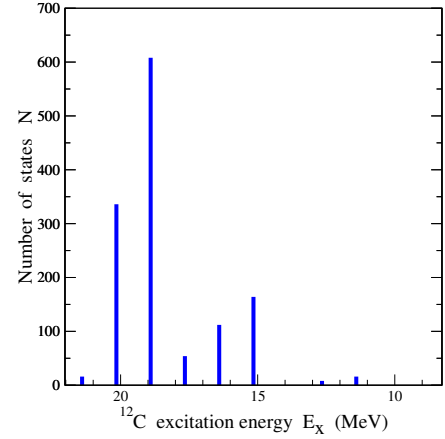


FIG. 6. (color online). Number of toroidal states as a function of the excitation energy E_x relative to the ground state for the ^{12}C nucleus in a toroidal configuration.

The experimental excitation function in Fig. 5 provides valuable information on the number of excited $^{12}\text{C}^*$ states as a function of E_x . It indicates that the number of $^{12}\text{C}^*$ states at $E_x \sim 10\text{--}20 \text{ MeV}$ that decay into 3α is very large. Above the Hoyle state energy, the toroidal particle-hole excitations built on the Hoyle state provide the dominant contribution to the number of states, on account of the extended geometrical size of the Hoyle state. It is illuminating to compare the number of toroidal particle-hole states as a function of E_x with the general behavior of the excitation function for $^{12}\text{C}^*$ production in Fig. 5. To facilitate such a comparison, we have plotted the number of toroidal states as a function of ^{12}C excitation energy E_x in Fig. 6 along the direction of decreasing E_x . The number of toroidal states is quite large at $E_x \sim 18\text{--}20 \text{ MeV}$ and has a smaller peak at $\sim 15\text{--}16 \text{ MeV}$. Experimental excitation function in Fig. 5 has a large peak at about 18 MeV and a substantial yield at around 16 MeV. There appears to be a qualitative correlation between the shape of the experimental excitation function with the theoret-

ical variation of the number of toroidal states, but more work is needed to make a quantitative comparison.

From the above comparisons outlined in subsections A, B, C, and D, there appear to be an approximate agreement of many pieces of data with the signatures of the ^{12}C nucleus in the toroidal configuration, but there are also many items that need to be further investigated to confirm the presence of such a toroidal configuration. Subject to these further experimental and theoretical tests that are opened up by such the new suggestion, the Hoyle state and many of its excited states may be tentatively identified as states of the ^{12}C nucleus in the toroidal configuration.

VI. TOROIDAL ^{12}C IN TOROIDAL CONSTRAINT DYNAMICS

Our investigation points to the need to devise tools within the mean-field theory that can constrain the nucleus so to possess local toroidal energy equilibrium configurations. We should be prepared to examine the toroidal configuration as excited diabatic states of the system. Success for formulating such tools will be useful not only for the ^{12}C nucleus but also for the many diabatic states that may be associated with the large region of toroidal high-spin isomers in α -conjugate nuclei up to $A \leq 70$ [74–76]. It will also be useful for the investigation of diabatic toroidal states in the intermediate and superheavy mass region for which some recent progress has been made [88–90].

We consider a Hamiltonian H_0 which contains already many constraints that have been imposed on the system. We wish to impose an additional toroidal constraint to hold the nucleus in a toroidal shape. For this purpose, we introduce a radial moment σ_ρ^2 to characterize the radial property of the density distribution that can constrain the density into a toroidal shape,

$$\sigma_\rho^2 = \left\{ \int d\mathbf{r} \, n(\mathbf{r}) (\rho - \langle \hat{\rho} \rangle)^2 \right\}, \quad (14)$$

where $\langle \hat{\rho} \rangle$ is the expectation value of the coordinate $\hat{\rho} = \rho = \sqrt{x^2 + y^2}$,

$$\langle \hat{\rho} \rangle = \int d\mathbf{r} \sum_{i=1}^A \psi_i^*(\mathbf{r}) \hat{\rho} \psi_i(\mathbf{r}), \quad (15)$$

and $n(\rho, z)$ is the nuclear density which can be determined self-consistently from the set of the wave functions $\{\psi_i\}$ of occupied states

$$n(\mathbf{r}) = \sum_{i=1}^A \psi_i^*(\mathbf{r}) \psi_i(\mathbf{r}). \quad (16)$$

The constraint of a fixed toroidal radial moment σ_ρ^2 , can be imposed with the additional Lagrange multiplier λ ,

$$H = H_0 + \lambda \left\{ \int d\mathbf{r} \, n(\mathbf{r}) (\rho - \langle \hat{\rho} \rangle)^2 - \sigma_\rho^2 \right\} \quad (17)$$

Upon a minimization of the Hamiltonian H with respect to a variation in ψ_i^* , we have

$$\frac{\delta H}{\delta \psi_i^*} = \frac{\delta H_0}{\delta \psi_i^*} + \lambda \int d\mathbf{r} \, (\rho - \langle \hat{\rho} \rangle)^2 \psi_i + (\text{terms involving } \frac{\delta \langle \hat{\rho} \rangle}{\delta \psi_i^*}) \quad (18)$$

To the extent that the change of the bulk $\langle \hat{\rho} \rangle$ with respect to the change of individual single-particle states ψ_i^* is small when the occupation numbers of the states have settled down and do not change, the last term of the above variation can be neglected. Writing H_0 in terms of the single-particle Hamiltonian h_0 as

$$H_0 = \int d\mathbf{r} \sum_{i=1}^A \psi_i^*(\mathbf{r}) h_0 \psi_i(\mathbf{r}), \quad (19)$$

and we have

$$\frac{\delta H_0}{\delta \psi_i^*} = \int d\mathbf{r} \, h_0 \psi_i. \quad (20)$$

Under the toroidal constraint of Eq. (17), the minimization of H with respect to ψ_i^* leads to the single-particle Hamiltonian under the toroidal constraint

$$h' = h_0 + \lambda (\rho - \langle \hat{\rho} \rangle)^2. \quad (21)$$

In the case with a large R/d ratio, $\langle \hat{\rho} \rangle \sim R$. Thus, we observe that the last term of Eq. (21) is approximately in the same form as the toroidal potential of Ref. [67], with the Lagrange multiplier λ playing the role of the harmonic oscillator frequency ω_\perp^2 multiplied by the nucleon mass m . We obtain the result that with the addition of the toroidal constraint Eq. (14), the variation principle lead to a single-particle toroidal potential that is similar to the potential of [66, 67] with the ω_\perp appearing as a variational parameter. For a given quadruple moment that leads to the proper R , the variation λ will lead to the proper radial width d of the transverse degree of freedom.

Another approach to examine toroidal nuclei can be carried out in diabatic mean-field calculations [71]. This is achieved by constraining the occupation of the single-particle states so that at the locations of the crossing of two single-particle states at the top of the fermi surface, one does not choose to occupy the state of the lowest energy. Instead, one maintains the diabatic configuration with the occupation of the state with the highest overlap with the earlier state before the level crossing, leading to a diabatic energy equilibrium as in [71]. Diabatic calculations have been performed successfully for ^{24}Mg [71] and ^{28}Si [70].

It will be of interest to see whether constraint dynamics or diabatic calculations for ^{12}C will reveal the toroidal ^{12}C states as discussed here. Although such constraint dynamics and diabatic calculations may appear simple in theoretical formulation, their implementation onto the self-consistent mean-field computer program are difficult tasks. We shall examine the microscopic mean-field description using the simpler method with variational wave functions.

VII. MICROSCOPIC DESCRIPTION OF ^{12}C STATES USING VARIATIONAL WAVE FUNCTIONS

The phenomenological analysis in Section V suggests the possibility that the Hoyle state and many of its low-lying excited states may be tentatively attributed to the particle-hole excitation of the ^{12}C nucleus from a toroidal configuration. It is therefore of great interest to search for the microscopic foundation for such a toroidal description for the Hoyle state as the band head of the particle-hole excitations, starting with the mean-field approximation using the Skyrme energy-density functional [78–80].

Assuming a ^{12}C nucleus with an intrinsic axial symmetry, we describe the states of the nucleus by a Slater determinant of neutrons and protons occupying the lowest-energy single-particle states $|n_\rho, n_z, \Lambda_z, \Omega_z\rangle$. For ^{12}C , the lowest-energy single-particles states are $|0, 0, 0, \pm 1/2\rangle$, $|0, 0, 1, \pm 3/2\rangle$, and $|0, 0, 1, \pm 1/2\rangle$. Limiting our considerations to $n_\rho=0$ and $n_z=0$ states, we shall omit the labels of “ $n_\rho=0$ ” and “ $n_z=0$ ” for brevity of notation. The variational parameters (R, d_ρ, d_z) of the single-particle wave functions will be so chosen that they allow the examination of the energy surface of the nucleus in many different configurations : the spherical, prolate spheroid, oblate spheroid, bi-concave disks, and toroidal configurations. For simplicity, we shall assume the same set of spatial and spin wave functions for neutrons and protons and neglect the spin-orbit interaction so that the radial wave function $\mathcal{R}_{\Lambda_z \Omega_z}$ of the single-particle state $|\Lambda_z \Omega_z\rangle$ depends only on Λ , the absolute value of Λ_z . The wave functions of the occupied single-particle states for a proton or a neutron can be represented in terms of the variation parameters (R, d_ρ, d_z) by

$$\Psi_{\Lambda_z \Omega_z}(\rho, z, \phi) = \mathcal{R}_\Lambda(\rho) Z(z) [\Phi_{\Lambda_z}(\phi) \chi_{s_z}]^{\Omega_z}, \quad (22a)$$

$$\text{where } \mathcal{R}_\Lambda(\rho) = N_\Lambda \rho^\Lambda \exp \left\{ -\frac{(\rho - R)^2}{2(d_\rho^2/\ln 2)} \right\}, \quad (22b)$$

$$Z(z) = N_Z \exp \left\{ -\frac{z^2}{2(d_z^2/\ln 2)} \right\}, \quad (22c)$$

$$\Phi_{\Lambda_z}(\phi) = \frac{e^{i\Lambda_z \phi}}{\sqrt{2\pi}}. \quad (22d)$$

In Eq. (22b), the parameter R describes approximately the position of the peak of the wave function in the radial coordinate¹. The ρ^Λ dependence of $\mathcal{R}_\Lambda(\rho)$ in Eq. (22b) arises from the behavior of the wave function near the origin at $\rho \rightarrow 0$, as inferred from the single-particle wave equation (2). The quantities d_ρ and d_z are related to the width of the wave function along the ρ and z direction

on the meridian plane. The normalization constants N_Z and $N_\Lambda(R, d_\rho)$ are given by

$$N_Z = \frac{1}{(2\pi d_z^2/2\ln 2)^{1/4}}, \quad (23a)$$

$$N_\Lambda(R, d_\rho) = \frac{1}{\sqrt{I^{(2\Lambda+1)}(t_0)}}, \quad (23b)$$

where

$$I^{(2\Lambda+1)}(t_0) \equiv \int_0^\infty d\rho \rho^{2\Lambda+1} \exp \left\{ -\frac{(\rho - R)^2}{(d_\rho^2/\ln 2)} \right\} \quad (24)$$

$$= \left(\frac{d_\rho}{\sqrt{\ln 2}} \right)^{2\Lambda+2} \frac{\sqrt{\pi}}{2} (2\Lambda + 1)! i^{(2\Lambda+1)} \text{erfc}(t_0),$$

and $i^{(2\Lambda+1)} \text{erfc}(t_0)$ is the integral of the error function as defined in Eq. (7.2.3) of [91],

$$i^{(2\Lambda+1)} \text{erfc}(t_0) = \frac{2}{\sqrt{\pi}} \int_{t_0}^\infty \frac{(t - t_0)^{(2\Lambda+1)}}{n!} e^{-t^2} dt \quad (25a)$$

$$\text{and } t_0 = -\frac{R}{d_\rho/\sqrt{\ln 2}}. \quad (25b)$$

The wave functions $\Psi_{\Lambda_z \Omega_z}(\rho, z, \phi)$ in Eq. (22a) for different quantum numbers $\{\Lambda_z, \Omega_z\}$ are orthonormal.

Instead of the (d_ρ, d_z) parameters, it is convenient to introduce their geometrical mean, $d = \sqrt{d_z d_\rho}$, and the dimensionless deformation parameter a_2 to write them as

$$d_z = d e^{+a_2}, \quad (26a)$$

$$d_\rho = d e^{-a_2}. \quad (26b)$$

The set of (R, d, a_2) parameters give rise to nuclear equidensity surfaces of different shapes:

- $R=0, a_2=0$: spherical surface,
- $R=0, a_2>0$: prolate spheroid,
- $R=0, a_2<0$: oblate spheroid,
- $R>0, a_2=0$: spheroid, bi-concave disk, toroid,
- $R<0, a_2<0$: oblate surface,
- $R<0, a_2>0$: prolate surface.

VIII. ^{12}C GROUND STATE ENERGY AND DENSITY DISTRIBUTION

We construct a Slater determinant for the occupied states and utilize the Skyrme SkM* interaction [80] to obtain the energy of the system as a function of the variation parameters (R, d, a_2) . With the variational wave functions Eqs. (22a)-(22d) for neutrons and protons, we get the nuclear density $n(\rho, z)$

$$n(\rho, z) = f_\phi f_\rho f_z, \quad (27a)$$

where

$$f_\phi = \frac{1}{2\pi}, \quad (27b)$$

$$f_\rho(\rho) = 4|\mathcal{R}_0(\rho)|^2 + 8|\mathcal{R}_1(\rho)|^2, \quad (27c)$$

$$f_z(z) = |Z(z)|^2. \quad (27d)$$

¹ Note that the symbol R here in the microscopic description in Eq. (22b) and the same symbol R in the phenomenological description in Eq. (3) represent different measures of the major toroidal radius and are different physical quantities, which can be easily distinguished by the context.

The kinetic energy density $\tau(\rho, z)$ defined as [78, 79]

$$\tau(\rho, z) = \sum_{\text{occ states}} |\nabla \psi_{\Lambda_z \Omega_z}(\rho, z)|^2,$$

is therefore

$$\begin{aligned} \tau(\rho, z) = & f_\phi f_\rho(\rho) |\nabla_z Z(z) \cdot \nabla_z Z(z)| \\ & + f_\phi f_z(z) \left\{ 4 |\nabla_\rho \mathcal{R}_0(\rho)|^2 + 8 |\nabla_\rho \mathcal{R}_1(\rho)|^2 \right. \\ & \left. + 8 \frac{\Lambda_z^2}{\rho^2} |\mathcal{R}_1(\rho)|^2 \right\}. \end{aligned} \quad (28)$$

The expectation value of the energy $E(R, d, a_2)$ of the ^{12}C nucleus in the mean-field approximation is therefore [78, 79]

$$\begin{aligned} E = \langle H \rangle = & \int 2\pi\rho d\rho dz \tau(\rho, z) \\ & + \int 2\pi\rho d\rho dz \left\{ \frac{3}{8}t_0 n^2 + \frac{1}{16}t_3 n^{\alpha+2} \right. \\ & \left. + \frac{1}{16}(3t_1 + 5t_2)n\tau + \frac{1}{64}(9t_1 - 5t_2)|\nabla n|^2 \right\} \\ & + \frac{1}{2} \int d^3r_1 d^3r_2 n(\mathbf{r}_1)n(\mathbf{r}_2) \frac{e^2}{|\mathbf{r}_1 - \mathbf{r}_2|}, \end{aligned} \quad (29)$$

where the Skyrme SkM* parameters are $t_0 = -2645 \text{ MeV} \cdot \text{fm}^3$, $t_1 = 410 \text{ MeV} \cdot \text{fm}^5$, $t_2 = -135 \text{ MeV} \cdot \text{fm}^5$, $t_3 = 15595 \text{ MeV} \cdot \text{fm}^6$, and $\alpha = 0.167$ [80].

With the quantities $n(\rho, z)$ and $\tau(\rho, z)$ given in terms of the wave functions, which are explicit functions of the variational parameters, the energy surface $E(R, d, a_2)$ is a function of the variational parameters. We first study the landscape of the energy surface $E(R, d, a_2)$ of ^{12}C among the nuclear shapes of the sphere, prolate spheroid, and oblate spheroid. This can be achieved by constraining R to be zero and making variations in d and a_2 . The contours of the energy surface $E(R, d, a_2)|_{R=0}$ on the (d, a_2) plane are given in Fig. 7.

As inferred from Fig. 7 for $R = 0$, the energy minima at $d = 1.49 \text{ fm}$ and $a_2 = -0.089$ occurs at $E_{R=0} \equiv E_0 = -66.68 \text{ MeV}$. The contribution of the spin-orbit interaction to the ground state of ^{12}C is -23.56 MeV from self-consistent Hartree-Fock calculations [60]. If the spin-orbit interaction is included, the total energy of the system will be -90.1 MeV which is close to the experimental value of -92.16 MeV .

We can examine the ground state nuclear density as shown in Fig. (8a) on the $y=0$ plane, and in Fig. (8b) on the $z=0$ plane. We note from Fig. (8a) that the shape of an equidensity surface of the ^{12}C ground state depends on the density value. The equidensity surfaces in the low density region are nearly oblate ellipsoids. The ratio of the axis length along the ρ -direction to the axis length in the z -direction at the half-density surface is approximately 2:1, as would be expected for the doubly magic

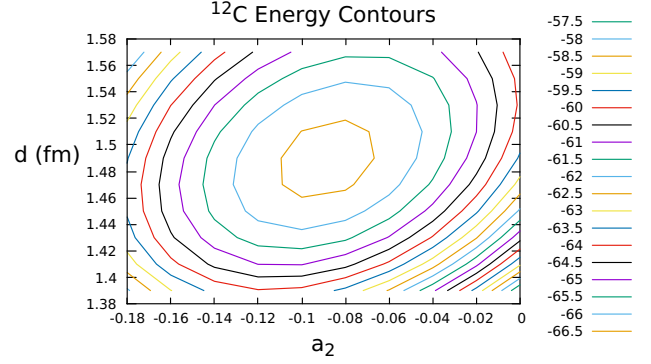


FIG. 7. (color online). The contours of the ^{12}C energy surface $E(R, d, a_2)|_{R=0}$ for $R = 0$ on the (d, a_2) plane. The ground state energy minimum appears at $d = 1.49 \text{ fm}$ and $a_2 = -0.089$ at an energy $E = E_0 = -66.68 \text{ MeV}$. The energy contours values labeled on the right are in units of MeV.

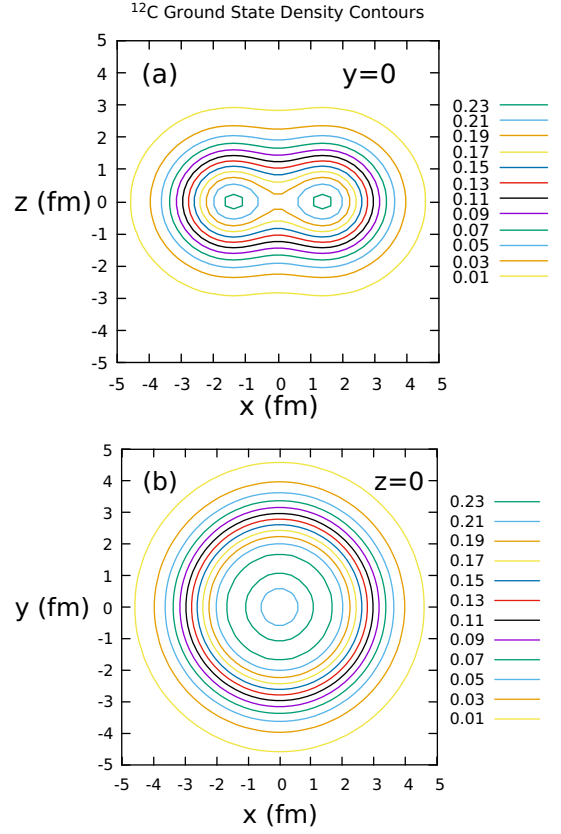


FIG. 8. (color online). The nuclear density of the ^{12}C ground state (a) on the $y = 0$ plane, and (b) on the $z = 0$ plane. The density contours labeled on the right are in units of $\text{nucleon}/\text{fm}^3$.

shell of $N = 6$ and $Z = 6$ in an anisotropic harmonic oscillator potential [66], in agreement with the experimental deformation of $\beta_2 = -0.6$ deduced in the direct reaction in neutron scatterings [77]. As the density increases, the equidensity surfaces turn into a bi-concave disks with a small indentation in the polar regions. When the den-

sity reaches $n \geq 0.21 \text{ /fm}^3$, the equidensity surfaces turn into toroids. Upon defining a toroidal nucleus as one in which some equidensity surfaces are toroidal, the ground state of the ^{12}C nucleus can be called a toroidal nucleus. It has a dense toroidal core immersed in lower-density oblate ellipsoids on the surface.

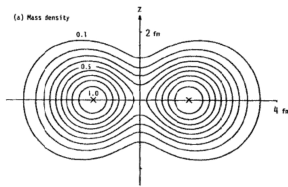
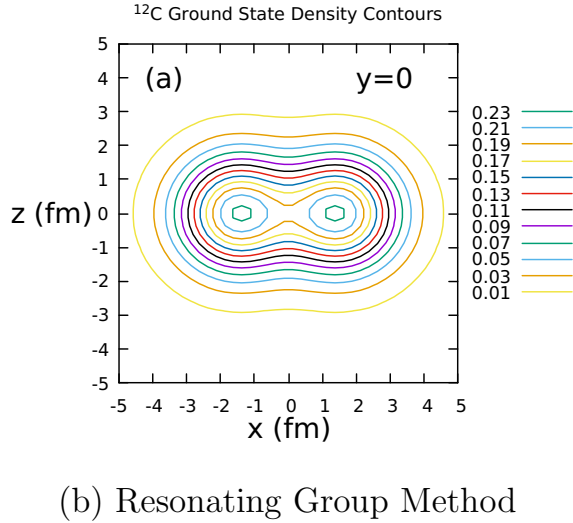


FIG. 9. (a) The nuclear density of the ^{12}C ground state on the $y=0$ plane obtained by minimizing the energy in the variations of (R, d, a_2) . The density contours are labeled in units of nucleon/ fm^3 . The density contours labeled on the right are in units of nucleon/ fm^3 . (b) The nuclear density n of the ^{12}C ground state on the $y=0$ plane obtained by the resonating group method (Fig. 4 of Kamimura [33]). The density contours are labeled in units of $1/10$ of the maximum density.

It should be pointed out that the toroidal feature of the ^{12}C nucleus of the ground state as exhibited in Figs. 8(a) and 9(a) may appear surprising, but it is in fact in agreement with earlier results from the resonating group method presented in Fig. 4 of Kamimura [33] and reproduced in our Fig. 9(b), where the density contours are given in units of $1/10$ of the maximum nuclear density. In the language of the generator coordinates and resonating groups, the toroidal density distribution in Fig. 9(b) arises from a generator coordinate superposition of the orientation of Wheeler’s triangular cluster wave functions on the cluster plane that generates naturally an intrinsic toroidal density. In the language of the nuclear shell effects [66–68], the toroidal feature of the inner core in Fig. 9(a) arises from the variation of the shape of the single-particle wave functions to reach the state of the lowest energy, and the lowest energy is obtained by set-

ting onto the doubly-closed toroidal shells of $N=Z=6$ [66, 67] resulting in a toroidal density. From such a perspective, there appears to be a high degree of equivalence and complementarity between the toroidal mean-field description emphasized here and Wheeler’s triangular 3α cluster description investigated elsewhere [21, 23–36].

In VAP (Variation after Projection) calculations in the triangular 3α cluster models for the ground state and the Hoyle state, the variation of the wave function is carried out after projecting out the $I=0$ and $M=0$ state from the triangular 3α cluster. The projection involves the superpositioning of the orientations of the triangular 3α clusters on the triangular plane, and the intrinsic nuclear density after projection is in essence a toroidal density, as the results of [33] in Fig. 9(b) demonstrate. The variation after the projection is therefore concerned with the stability of the nucleus under the variation of an intrinsic toroidal density. In VAP calculations for the ^{12}C ground state in the resonating group method [33], the solution of the Wheeler’s triangular cluster is compact, and the corresponding toroidal dense core is immersed in lower-density oblate spheroids. In VAP calculations for the Hoyle state, the AMD and FMD solutions of Wheeler’s triangular cluster have a greater spatial extension [22, 43–48], as is also indicated by experimental inelastic scattering experiments [92]. It is reasonable to expect a toroidal nucleus with a more prominent toroidal features and a larger toroidal major radius for the Hoyle state.

IX. ADIABATIC ENERGY $E(R)$ ABOVE THE GROUND STATE

To study the properties of the low-lying excited states above the ground state, we examine the energy surface and the nuclear density distributions for different values of R around the ground state of ^{12}C . Under the constraint of a major radius parameter R , we look for the lowest “adiabatic” energy $E(R)$ by searching for the (d, a_2) values that lead to an energy minimum. For a constrained value of R in question, the adiabatic energy $E(R)$ is determined by the minimum energy on the (d, a_2) plane.

Figure 10 gives the adiabatic energy $E(R)$ as a function of R and Table VII lists the corresponding equilibrium location (d, a_2) at the energy minimum and the excitation energy $E_x(R) = E(R) - E_0$, where $E_0 = E_{R=0}$. As R increases, the equilibrium minor radius d decreases, and the equilibrium deformation parameter a_2 increases. The meridian cross section changes from an oblate shape to a nearly circular shape on the meridian plane, as R increases. In the region of negative value of R , the adiabatic system have nearly the same shape as the oblate nucleus at $R=0$. Hence the adiabatic energy flattens out in the region of negative R .

We find in Table VII and Fig. 10 that the ground state energy E_0 at $R = 0$ is a minimum not only under the variation of (d, a_2) but also a minimum under a variation of R . Fig. 10 shows further that as a function of R there

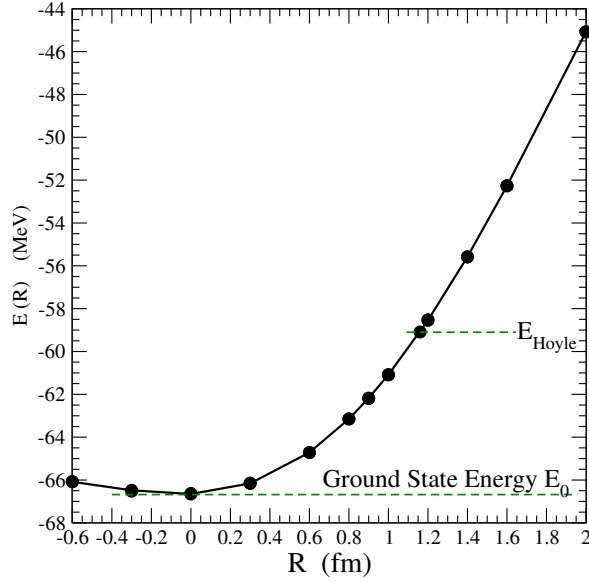


FIG. 10. (color online). The solid points and the adjoining solid line give the adiabatic energy $E(R)$ of ^{12}C . For each value of R , the energy $E(R)$ is determined as the minimum of the energy in the (d, a_2) plane, whose location at the minimum is listed in Table VII.

is no additional local energy minimum at a non-zero positive value of R in the mean-field approximation.

TABLE VII. For each value of R , the energy $E(R)$ is the minimum of the energy on the (d, a_2) plane, for which the (d, a_2) location at the minimum are listed. The excitation energy E_x is the energy $E(R)$ relative to the ground state E_0 , $E_x = E(R) - E_0$, where $E_0 = E_{R=0}$.

R (fm)	$E(R)$ (MeV)	E_x (MeV)	d (fm)	a_2
-0.60	-66.07	0.61	1.570	-0.140
-0.30	-66.52	0.16	1.540	-0.120
0.0	-66.68	0.00	1.493	-0.089
0.3	-66.14	0.54	1.450	-0.065
0.6	-64.72	1.96	1.420	-0.050
0.9	-62.20	4.48	1.394	-0.025
1.0	-61.09	5.59	1.377	-0.020
1.16	-59.03	7.65	1.370	-0.007
1.2	-58.52	8.16	1.368	-0.004
1.4	-55.59	11.09	1.360	0.004
1.6	-52.26	14.42	1.354	0.010
2.0	-45.08	21.60	1.350	0.020

We can examine the energy surface in other degrees of freedom in order to search for a secondary local energy minimum. The toroidal shape density can evolve into a 3α cluster distribution by the sausage deformation σ_3 of order $\lambda = 3$, which turns an azimuthal-symmetric toroid into three clusters with three adjoining necks, (as illustrated in Fig. 3 of Ref. [67]). To study the question of stability with respect to a variation in σ_3 , we modify the

wave function $\Phi_{\Lambda_z}(\phi)$ of Eq. (22d) to

$$\Phi_{\Lambda_z}(\phi) = \frac{(1 + \sigma_3 \rho^3 e^{3i\phi}) \rho^\Lambda e^{i\Lambda_z \phi}}{\sqrt{2\pi}}. \quad (30)$$

Direct calculations in the mean-field theory with Skyrme SkM* interactions reveal that in the neighborhood of the Hoyle energy region the toroidal state, Ψ_{toroid} , the nucleus system is stable against sausage deformation of order $\lambda=3$ at $\sigma_3 = \sigma_{3T} = 0$. There is no local energy minimum at a non-zero value of σ_3 and R as shown in Fig. 11. We can further explore different R_Λ param-

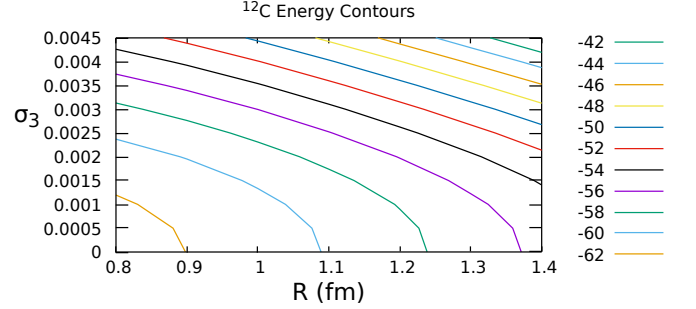


FIG. 11. (color online). The energy contours of the energy surface $E(R, \sigma_3)$ in the plane of (R, σ_3) for the set of parameters $d=1.370$ fm and $a_2=-0.007$ appropriate for the excitation energy at the Hoyle energy. The energy contours are labeled in units of MeV.

ters for the different Λ single-particle states. Upon considering the parameters space of $(R_{\Lambda=0}, R_{\Lambda=1}, d, a_2, \sigma_3)$, we find that in the mean field approximation with the Skyrme SkM* interaction, there is only a single ground state energy minimum at $(R_{\Lambda=0}, R_{\Lambda=1}, d, a_2, \sigma_3) = (0, 0, 1.493\text{fm}, -0.089, 0)$, with no secondary local energy minimum in the neighborhood of the Hoyle energy. Extensive Hartree-Fock and Hartree-Fock-Bogoliubov calculations using the Skyrme SkM* interactions also fails to indicate a secondary toroidal local energy minimum in the neighborhood of the Hoyle energy [60].

X. DENSITY DISTRIBUTION OF THE ^{12}C NUCLEUS AT HOYLE ENERGY

A. Toroidal State Ψ_{toroid} at Hoyle Energy

The adiabatic energy $E(R)$ examined in Fig. 10 and listed in Table VII allows us to find the variational parameter values (R, d, a_2) at which the ^{12}C excitation energy is at the Hoyle excitation energy. From Table VII, we find that the case of $(R=1.16$ fm, $d=1.370$ fm, $a_2=-0.007)$ corresponds to an excitation energy of the Hoyle energy at $E_x=7.65$ MeV. With this set of variational parameters, we can calculate the nuclear density distribution of the state of the system at the Hoyle energy. We plot the nuclear density on the x - z plane at $y=0$ in Fig. 12(a) and the density contours on the x - y plane

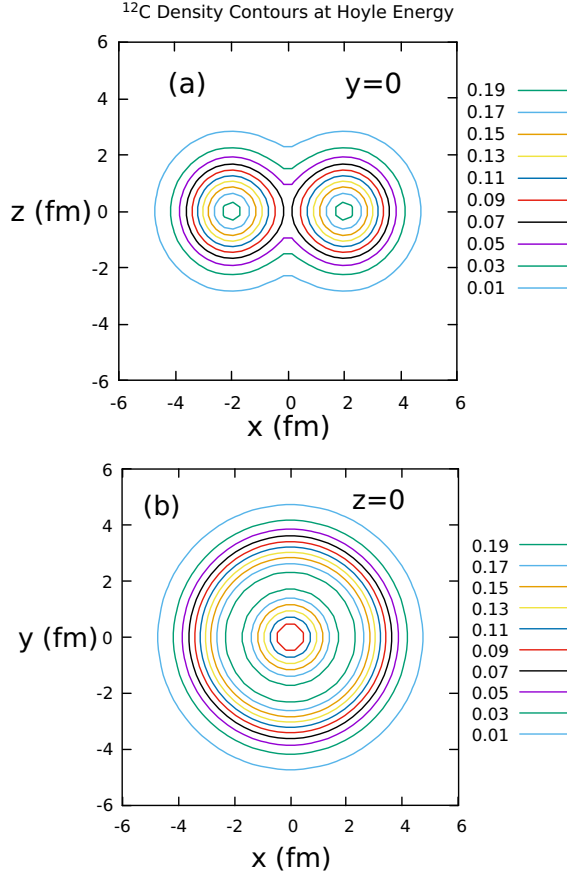


FIG. 12. (color online). The nuclear density for the toroidal state of ^{12}C at the Hoyle state excitation energy, (a) on the $z=0$ plane, and (b) on the y plane. The density contours are labeled in units of nucleon/ fm^3 .

at $z=0$ in Fig. 12(b). One observes that for this state of the system at the Hoyle energy on the $E(R)$ energy surface, the equidensity surfaces with density $n \geq 0.07/\text{fm}^3$ appear as separated toroids, while those with lower densities as spindle toroids. The meridian cross sections are nearly circular. Thus, the toroidal core that shows up for the ^{12}C ground state at $R=0$ becomes much more prominently toroidal, as R increases to $R=1.16$ fm at the Hoyle energy region. One concludes from such an investigation that there is a state at the Hoyle energy with a prominent toroidal density distribution shown in Fig. 12 that is degenerate with the energy of the Hoyle state. It is a Slater determinant consisting of single-particles states of Eqs. (22a-22d) with the appropriate R , d , and a_2 values. In the mean-field theory, such a state is stable against variations in d and a_2 but lies on an energy slope as a function of $E(R)$, as shown in Fig. 10. It is therefore unstable against the contraction of the major radius R in the mean-field approximation. We nonetheless call it a provisional toroidal state at the Hoyle energy, Ψ_{toroid} , on account of its toroidal density shape, pending further investigation of its stability against R variations. We shall examine whether many-body interactions beyond

the mean field may affect the stability of the provisional toroidal state Ψ_{toroid} against variations in R . It should however be kept in mind that pending modifications arising from additional interactions beyond the mean field may modify slightly the R location and the shape of the density distribution but will not likely change its toroidal characteristics.

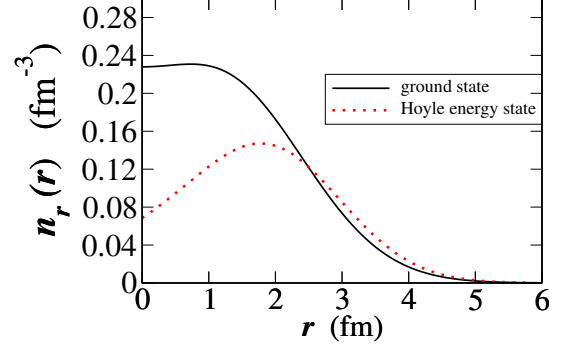


FIG. 13. The nuclear density $\rho(r)$ in the spherical coordinate system, after integrating over the polar angles. (a) Results from the antisymmetric molecular dynamics calculations of [46], and (b) from the provisional toroidal state at $R = 1.16$ fm, Ψ_{toroid} , at the Hoyle energy.

We can get another idea on the spatial extension of the ground state and the provisional toroidal state Ψ_{toroid} plot the density distribution $n_r(r)$ of Ψ_{toroid} as a function of the spherical radial coordinate r after integrating over the polar angle θ ,

$$n_r(r) = \int_0^\pi n(\rho, z) \sin(\theta) d\theta, \quad (31)$$

for which $2\pi \int n_r(r) r^2 dr = A$. The angle-integrated densities $n_r(r)$ as a function of the spherical coordinate r for the ground state (with $R = 0$) and the provisional toroidal state at Hoyle energy (with $R=1.16$ fm) are plotted in Fig. 13. We note that the density $n_r(r)$ in the interior of the ground state is about two to three times that of the provisional toroidal state Ψ_{toroid} , but the latter has a more extended distribution at large r values.

B. Models of 3α Clusters

Even though we do not find a toroidal local energy minimum as a function of R in the mean-field theories, we are however motivated to continue the search in view of the many pieces of experimental evidence supporting the tentative identification the Hoyle state and many of its excited states to be states of ^{12}C in a toroidal configuration, as discussed in Section V. From intuitive viewpoints, we are further encouraged by the small energy separation between the Hoyle state and its excited states, by the large number of both the identified and the un-identified broad excited states, by the close average energy spacing between the states, and by their predominance in their

decay into three alpha particles. These characteristics suggest that the Hoyle state is intrinsically a spatially extended object that is capable of possessing a complex particle-hole excitation structure. A toroidal description is consistent with such a suggestion. Theoretically we find it promising that the ground state nuclear density as exhibited in Fig. 8 already shows a toroidal structure in its core and the provisional state at the Hoyle energy in Fig. 12 exhibits prominent toroidal characteristics. We also note with interest that there may be residual interactions beyond the mean-field that may be peculiar to ^{12}C and have important effects on the stability of the toroidal system as a function of R .

We seek guidance from earlier models that have been successful in describing both the ground state and the Hoyle state. Cluster models of different types, originating from Wheeler's concept of a triangular cluster of three alpha particles, have been quite successful in explaining many salient features of the states of the ^{12}C nucleus. There is the interacting cluster model of three alpha particles in which the alpha particles are approximated to be structure-less for simplicity but the dynamics of the clusters are solved as a quantum mechanical three-body problem [23–26]. There are the resonating group method [1, 2, 33] and the generator coordinate method of alpha clusters [21, 28–30] in which the nucleons and their exchanges are described microscopically and the dynamics between clusters is determined by a variational principle with the variational wave function as a superposition of triangular 3α clusters wave function. The ground state and the Hoyle state appear as quantized solutions of the Hill-Wheeler equation appropriate for a system of three alpha particles with different radial extensions. In addition, there are also the AMD model [43–46] and the FMD model [22, 47, 48] in which the cluster states and the shell model states coexist, and the nucleons cluster automatically by themselves upon a minimization of the energy of the system.

All the above mentioned models find the ground state and the Hoyle state as 3α clusters, with the Hoyle state to be spatially more extended than the ground state. Although the ground state may be adequately described by the independent particle mean-field theory, the description of the Hoyle state in all these descriptions appears to require effectively interactions beyond the mean field.

We shall discuss the simplest cluster model of Ref. [23–26] as a representative, in order to bring out the most important ingredients. In this cluster model of ^{12}C as a quantum-mechanical three-body problem with structure-less alpha particles, the two-alpha interaction is taken from a phenomenological Ali-Bodmer interaction that describes well the properties of the two-alpha systems [93]. It was found that good agreement of the properties of the low-lying states and their decay widths [23–26] necessitates the introduction of an attractive three-alpha cluster interaction taken to be of the form

$$V_{3\alpha}(\mathbf{r}_1\mathbf{r}_2\mathbf{r}_3) = S \exp\{-\rho^2/b^2\}, \quad (32)$$

where \mathbf{r}_i is the coordinate of the i th alpha particle and

$$\rho^2 = \frac{4}{3} \sum_{i<j}^3 (\mathbf{r}_i - \mathbf{r}_j)^2 / b^2. \quad (33)$$

The range parameter b has been taken to be 6 fm in [23–26], corresponding to the situation that the case of $\rho=b$ corresponds to the condition of three touching alpha particles. For the Hoyle state, S was found to be -20 MeV. The occurrence of the Hoyle state in the collision of three alpha particles in stellar evolution, leading to the nucleosynthesis from light elements to heavy elements, provides an additional strong support for the presence of this type of three-alpha cluster residual interaction.

In a completely microscopic picture including the constituents of the alpha particles, the three-alpha interaction such as Eq. (32) will involve all twelve nucleons that is beyond the scope of the mean-field approximation.

C. Possible Coexistence of the Toroidal and the Three-alpha Cluster Configurations

With the addition of the 3α cluster force, the quantum-mechanical three-body problem was solved to obtain the 3α cluster state $\Psi_{3\alpha}$ that gives a good description of the Hoyle state energy and decay width as described in [23–26]. We have thus the situation that there are two degenerate states with distinctly different density distributions but with the same energy : (i) the (provisional) toroidal state Ψ_{toroid} with a toroidal density distribution at the Hoyle energy as shown in Fig. 12, and (ii) the 3α cluster state $\Psi_{3\alpha}(\mathbf{r}_1\mathbf{r}_2\mathbf{r}_3)$ at the Hoyle energy as obtained in [23] by solving the three-body problem. They are degenerate at the Hoyle energy. Because of the energy degeneracy, the two states must mix with each other.

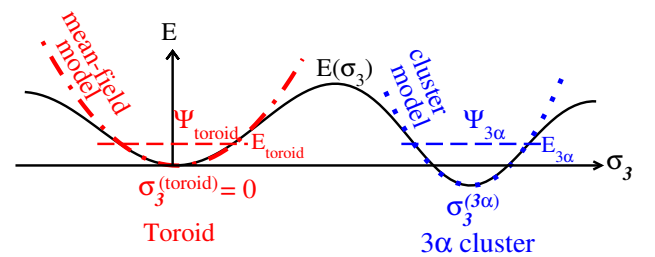


FIG. 14. (color online). Schematic depiction of the energy curve $E(\sigma_3)$ (solid curve) in the sausage degree of freedom, σ_3 at the Hoyle energy, $E_{\text{toroid}} = E_{3\alpha} = E_{\text{Hoyle}}$. The toroidal state Ψ_{toroid} is stable against σ_3 variations at $\sigma_3 = \sigma_3^{(\text{toroid})} = 0$. The 3α cluster state $\Psi_{3\alpha}$ is stable against σ_3 variations at $\sigma_3 = \sigma_3^{(3\alpha)}$. The two degenerate configurations mix with each other to give rise to a pair of states.

The toroidal shape density can evolve into a three- α cluster density by the sausage deformation σ_3 , of order $\lambda = 3$. We can envisage the behavior of the energy surface $E(\sigma_3)$ similar to those in a double-well potential

or a fission isomer [68, 94, 95], as shown schematically in Fig. 14. Direct calculations in a mean-field theory reveal in Fig. 11 that the toroidal state Ψ_{toroid} at the Hoyle energy is stable against sausage deformation of order $\lambda = 3$ at $\sigma_3 = \sigma_3^{(\text{toroid})} = 0$, as depicted schematically by the dashed-dot curve in Fig. 14. On the other hand, by including the essential three-alpha attractive interaction [Eq. (32)] in the quantum mechanical three-body problem, the 3α cluster model yields a resonance $\Psi_{3\alpha}$ at the Hoyle energy, with the correct three-alpha decay width [23]. The presence of such a 3α cluster state at the Hoyle energy means that the 3α cluster state is a local energy minimum at a non-zero value of $\sigma_3 = \sigma_3^{(3\alpha)}$, as depicted as the dotted curve in Fig. 14. Thus, there are two degenerate states, Ψ_{toroid} and $\Psi_{3\alpha}$, at the Hoyle energy. A complete solution will involve the full σ_3 space with both shapes to lead to the mixing of the two configurations, similar to the case of fission isomers [68] and shape isomerism in Hg isotopes [94]. A solution for two physical states in the full σ_3 space will be of the type

$$\Psi_I = a_{\text{toroid}} \Psi_{\text{toroid}} + a_{3\alpha} \Psi_{3\alpha}, \quad (34a)$$

as in a double-well potential and fission isomers [68, 94, 95]. The two states Ψ_{toroid} and $\Psi_{3\alpha}$ are not orthogonal as their overlap $\langle \Psi_{\text{toroid}} | \Psi_{3\alpha} \rangle$ is in general not zero. The Hamiltonian matrix for these two states needs to be constructed and diagonalized to obtain the pair of physical states. The splitting between the pair of two physical states involves a tunneling through the barrier between the toroidal state at $\sigma_3 = \sigma_3^{(\text{toroid})} = 0$ to the three-alpha cluster and the local energy minimum at a finite $\sigma_3^{(3\alpha)}$ [95].

D. Effective 3α Cluster Interaction beyond the Mean Field

The presence of the attractive three-cluster interaction $V_{3\alpha}$ such as that represented in Eq. (32) will lead to a correction to mean-field adiabatic surface $\Delta E_{3\alpha}(R)$ for the toroidal configuration. We envisage that the many-nucleon system leads to a physical state at the Hoyle energy that has a toroidal component $\Psi_{\text{toroid}}(R)$ described by a Slater determinant of the toroidal single-particle orbitals given in Eqs. (22a-22d). The effect of a three-alpha particle cluster interaction $V_{3\alpha}$ leads to a change of the adiabatic energy in the toroidal sector given by

$$\begin{aligned} \Delta E_{3\alpha}(R) &= \langle \Psi_{\text{toroid}}(R) | V_{3\alpha} | \Psi_{\text{toroid}}(R) \rangle \\ &= \int d\mathbf{r}_1 d\mathbf{r}_2 d\mathbf{r}_3 \langle \Psi_{\text{toroid}}(R) | \Psi_{3\alpha}(\mathbf{r}_1 \mathbf{r}_2 \mathbf{r}_3) \rangle^2 V_{3\alpha}(\mathbf{r}_1 \mathbf{r}_2 \mathbf{r}_3). \end{aligned}$$

Here, the three-alpha cluster state $\Psi_{3\alpha}(\mathbf{r}_1 \mathbf{r}_2 \mathbf{r}_3)$ is quantized in accordance with the three-body wave equation [23] and it has a definite root-mean-square radius. Therefore, the probability $|\langle \Psi_{\text{toroid}}(R) | \Psi_{3\alpha}(\mathbf{r}_1 \mathbf{r}_2 \mathbf{r}_3) \rangle|^2$ can be represented by a Gaussian with a width parameter a_R centered at the R_0 value, for which $\Psi_{\text{toroid}}(R_0)$ and the

solution $\Psi_{3\alpha}(\mathbf{r}_1 \mathbf{r}_2 \mathbf{r}_3)$ have the same root-mean-square radius. We are led to a semi-empirical adiabatic energy correction arising from the 3-alpha clustering interaction of the form

$$\Delta E_{3\alpha}(R) = A e^{-(R-R_0)^2/2a_R^2} \quad (35)$$

The set of parameters of $A=6$ MeV, $R_0=1.6$ fm, and $a_R=0.15$ fm will give a secondary toroidal energy minimum at the Hoyle energy of $E_x = 7.65$ MeV at $R=1.55$ fm. They serve here only as an example to indicate that there are known interactions beyond the mean field that may have important effects on the stability of the ^{12}C nucleus in the toroidal configuration at the Hoyle energy. Much more work will need to be carried out to clarify the situation. The phenomenological to investigate toroidal shape should continue to proceed because both the microscopic foundation and the phenomenology on the intrinsic shape of the Hoyle state will benefit from progress in either direction.

XI. CONCLUSIONS AND DISCUSSIONS

In spite of many investigations on the excited states of ^{12}C , the physical nature of the Hoyle state and its many excited states remains an interesting puzzle [7–21, 23–26]. We explore the toroidal degree of freedom for the reason that the ^{12}C nucleus, with 6 neutrons 6 protons, is a doubly closed-shell nucleus in a toroidal potential. A generator coordinate superposition of the orientations of Wheeler's triangular cluster states on the cluster plane will naturally generate a toroidal density. Many excited states of ^{12}C decays predominantly into three alpha particles, and a cluster of three alpha particles has a probability amplitude overlap with the toroidal wave function. Recently, experimental evidence for toroidal high-spin isomers in ^{28}Si predicted by a number of theoretical investigations have recently been reported [70]. For these reasons, we study the states of the ^{12}C nucleus in a toroidal configuration from both phenomenological and microscopical viewpoints.

In the phenomenological approach, we search for the signature of a toroidal nucleus and we find that the ^{12}C single-particle state energies have a simple Λ^2/R^2 structure and these states bunch together to form single-particle Λ -shells. Consequently the toroidal shell structure gives rise to particle-hole multiplets of ^{12}C excited states bearing the signature for the intrinsic toroidal properties. The spectrum of a toroidal nucleus is characterized by these shell-to-shell step-wise particle-hole excitation multiplets of various spin, parities, and excitation energies.

Upon comparing with the experimental spectrum, we find approximate agreement of the spins and parities of identified low-lying states. The underlying broad structures in the excitation functions of the $^{11}\text{B}(^3\text{He}, d)^{12}\text{C}^* \rightarrow 3\alpha$ reaction of Ref. [15] indicates the

possible presence of the remainder members of the produced multiplets. The $^{10}\text{B}(^3\text{He},p)^{12}\text{C} \rightarrow 3\alpha$ data at higher energies indicates possible copious production of toroidal states as a large underlying broad structure underneath the resolved resonances. Subject to further experimental and theoretical investigations, the Hoyle state and many of its excited states may be tentatively attributed to be states of a ^{12}C nucleus in the toroidal configuration, with the Hoyle state as the band head. There may be a large number of toroidal ^{12}C states over a large energy region that readily breakup into three alpha particles, which may have implications in energy-producing mechanisms.

In the microscopic mean-field approximation with the Skyrme energy density functional for the ^{12}C nucleus, we find that the ground state of ^{12}C has an low oblate spheroidal density distribution on the surface but a high density toroidal distribution in the core, in agreement with previous calculations using the generating coordinate method. At the Hoyle energy, the nuclear density exhibits a pronounced toroidal structure. On the other hand, previous quantum three-body treatment of the ^{12}C nucleus yields the proper resonance energy and width at the Hoyle energy when a three-body force is introduced [23, 24]. Because the toroidal state can evolve into a three-alpha cluster through the sausage deformation σ_3 and the toroidal state and the 3α cluster states have the same energy, the physical state is likely a mixture of the toroidal state and the 3α cluster state, suggesting the possibility of a toroidal coexistence of the physical state possessing probability amplitudes for both the toroidal and the three-alpha cluster configurations. The physical Hoyle state and many of its excited states may therefore exhibit toroidal nucleus characteristics with the presence of particle-hole multiplets examined here as well as three-alpha cluster characteristics studied in cluster models. Such a coexistence model is similar to the coexistence model [19, 34] proposed earlier. The difference is that the cluster model with shell model wave function is hereby replaced with a toroidal structure that is geometrical in its content.

It is instructive to compare and contrast the advantages and disadvantages in the toroidal and the three-alpha cluster descriptions of the ^{12}C nucleus under different physical probes in different measurements. In the toroidal configuration, nucleons traverse azimuthal orbitals and a particle-hole excitation can be promoted easily from one azimuthal Λ -shell to another Λ -shell with low expenses in energy, of order a few MeV. On the other hand, in the three-alpha cluster of strongly bound alpha particles as a dilute gas, a particle-hole excitation of the alpha particles will require a very high energy, of order 20 MeV. Hence, the toroidal configuration may be more efficient for problems involving particle-hole excitations, as for example, in the stripping-type experiments carried out in the Aarhus-Madrid Collaboration in [15–17]. In matters of the isolation of the four correlated particles as an escaping entity and the tunneling through the eter-

nal Coulomb barrier the three-alpha cluster configuration may provide a more convenient description. A toroidal coexistence picture of the ^{12}C nucleus as a mixing of both the toroidal and three-alpha cluster configurations may therefore be a useful concept.

The proposed toroidal description of the ^{12}C states may be useful not only to correlate existing experimental data, it has a number of predictions that will stimulate future experimental and theoretical work. Specifically, the toroidal particle-hole picture predicts many additional states in the particle-hole multiplet, and it is likely that these are the broad states in the underlying structure under the identified sharp states, as is discussed in Section V. Therefore, experimental identification of the spin and parity of the broad states in the underlying structure, if at all possible, will be useful. In this respect, recent experimental effort in finding the spin and parity of a broad state in the continuum can be of value [97]. Theoretically, it will also be of interest to plot the intrinsic nuclear density on the x - z plane for the Hoyle states in the GCM and RGM calculations or other microscopic calculations. The present work would predict that the Hoyle state will show an intrinsic toroidal density, just as the ground state shows an intrinsic toroidal dense core in the GCM work with a 3α cluster in the work of Kamimura [33] discussed in Section 10A. Theoretically, much work needs to be done to understand quantitatively the excitation function to see if the spectroscopic factors for the different states in the multiplets are indeed as they should be. We also need to understand theoretically why some states have narrow width while some other have broad width. Is it correlated with their toroid-like or 3-alpha-cluster-like behavior?

In future theoretical work, it will be necessary to include spin-orbit and other residual interactions so as to obtain the fine-structure of the multiplets. The knowledge of a better wave function will allow the evaluation of the toroidal moment of inertia of the Hoyle state, for comparison with the observed moment of inertia. How the additional three-alpha cluster interaction may be included as a residual interaction in a mean-field dynamics will be of great interest. The quantitative evaluation of the overlap amplitude between the toroidal state and the 3α cluster state and the correction to the adiabatic energy $\Delta E_{3\alpha}(R)$ arising from the three-alpha interaction will be of great interest to provide a firmer foundation on the microscopic description of the toroidal configuration.

Acknowledgments

The authors would like to thank Profs. Aksel S. Jensen, Larry Zamick, Yitzak Sharon, Ikuko Hamamoto, Jirina Stone, Hans O. U. Fynbo, Oliver S. Kirsebom, Soren Sorensen, Howard Holme, and Joe Natowitz for helpful communications and discussions. The research was supported in part by the Division of Nuclear Physics, U.S. Department of Energy under Contract DE-AC05-00OR22725.

-
- [1] J. A. Wheeler, *Molecular Viewpoint in Nuclear Structure*, Phys. Rev. **52**, 1083 (1937).
- [2] J. A. Wheeler, *On the Mathematical Description of Light Nuclei by the Method of Resonating Group Structure*, Phys. Rev. **52**, 1107 (1937).
- [3] D. N. F. Dunbar, R. E. Pixley, W.A. Wenzel, and W. Whaling, *The 7.68-MeV state in ^{12}C* , Phys. Rev. **92**, 649 (1953).
- [4] F. Hoyle, D. N. F. Dunbar, W.A. Wenzel, and W. Whaling, Phys. Rev. **92**, 1095c (1953).
- [5] F. Hoyle, *On Nuclear Reaction Occuring in Very Hot Stars*, Astrophys. J. Supplement, **51**, 121 (1954).
- [6] C. W. Cook, W. A. Fowler, and T. Lauritsen, Phys. Rev. **107**, 508 (1957).
- [7] C. Beck (Editor), Lecture Notes in Physics 848, *Clusters in Nuclei*, Springer Verlag, Berlin, 2010.
- [8] C. Wheldon, Tz. Kokalova, M. Freer, A. Glenn, D. J. Parker, T. Roberts, and I. Walmsley *States at high excitation in ^{12}C from the $^{12}\text{C}({}^3\text{He}, {}^3\text{He})3\alpha$ reaction*, Phys. Rev. **C90**, 014319 (2014).
- [9] T. K. Wheldon, *Over half a century of studying carbon-12*, J. Phys.: Conf. Ser. **639**, 012003 (2015).
- [10] R. Smith *et al.*, *New Measurement of the Direct 3α Decay from the ^{12}C Hoyle State*, Phys. Rev. Lett. **119**, 132502 (2017).
- [11] D. Dell'Aquila *et al.*, *High-Precision Probe of the Fully Sequential Decay Width of the Hoyle State in ^{12}C* , Phys. Rev. Lett. **119**, 132501 (2017).
- [12] W. R. Zimmerman *et al.*, *Unambiguous Identification of the Second 2^+ State in ^{12}C and the Structure of the Hoyle State*, Phys. Rev. Lett. **110**, 152502 (2013).
- [13] M. Gai, *Current and Future Tests of the Algebraic Cluster Model of ^{12}C* , J. Phys. Conf. Ser. **876**, 012009 (2017).
- [14] J.H. Kelley, J.E. Purcell, C.G. Sheu, *Energy levels of light nuclei $A = 12$* , Nucl. Phys. **A 968**, 71253 (2017).
- [15] O. S. Kirsebom, M. Alcorta, M. J. G. Borge, M. Cubero, C. A. Diget, R. Dominguez-Reyes, L. M. Fraile, B. R. Fulton, H. O. U. Fynbo, S. Hyldegaard, B. Jonson, M. Madurga, A. Muoz Martin, T. Nilsson, G. Nyman, A. Perea, K. Riisager, and O. Tengblad, *Breakup of ^{12}C resonances into three α particles*, Phys. Rev. **C81**, 064313 (2010).
- [16] O. S. Kirsebom, M. Alcorta, M. J. G. Borge, M. Cubero, C. A. Diget, L. M. Fraile, B. R. Fulton, H. O. U. Fynbo, D. Galaviz, B. Jonson, M. Madurga, T. Nilsson, G. Nyman, K. Riisager, O. Tengblad, and M. Turrión, *Improved Limit on Direct α Decay of the Hoyle State*, Phys. Rev. Lett. **108**, 202501 (2012).
- [17] Alcorta *et al.*, *Properties of ^{12}C resonances determined from the $^{10}\text{B}({}^3\text{He}, p\alpha\alpha\alpha)$ and $^{11}\text{B}({}^3\text{He}, d\alpha\alpha\alpha)$ reactions studied in complete kinematics*, Phys. Rev. **C81**, 064306 (2012).
- [18] M. Barbui, K. Hagel, J. Gauthier, S. Wuenschel, R. Wada, V. Z. Goldberg, R. T. deSouza, S. Hudan, D. Fang, X.-G. Cao, and J. B. Natowitz, *Searching for states analogous to the ^{12}C Hoyle state in heavier nuclei using the thick target inverse kinematics technique*, Phys. Rev. **C98**, 044601 (2018).
- [19] H. Horiuchi, *Coexistence of Cluster States and Mean-Field-Type States*, in Chap. V of , *Clusters in Nuclei*, (Ed. C. Beck), Springer Verlag, Berlin, 2010, p 57-107.
- [20] M. Freer, H. Horiuchi, Y. Kanada-En'yo, D. Lee, and U.-G. Meiner, *Microscopic Clustering in Nuclei*, Rev. Mod. Phys. **90**, 035004 (2018).
- [21] P. Descouvemont and M. Dufour, *Microscopic Cluster Models*, Vol. 2 of *Clusters in Nuclei*, C. Beck (ed.), Lecture Notes in Physics 848, Springer Verlag, Berlin, 2012.
- [22] H. Feldmeier and T. Neff, *Nuclear Clustering in Fermionic Molecular Dynamics*, in Book “Nuclear Particle Correlations and Cluster Physics”, Editor Wolf-Udo Schröder, pp. 71-94 (2017) [arxiv:1612.02602].
- [23] R. Álvarez-Rodríguez, E. Garrido, A. S. Jensen, D. V. Fedorov, H. O. U. Fynbo, *Structure of Low-Lying ^{12}C Resonances*, Euro. Phys. Jour. **A31**, 303-317 (2007).
- [24] R. Álvarez-Rodríguez, A. S. Jensen, D. V. Fedorov, H. O. U. Fynbo, E. Garrido *Energy Distributions from Three-Body Decaying Many-Body Resonances*, Phys. Rev. Lett. **99**, 072503 (2007).
- [25] R. Alvarez-Rodríguez, A. S. Jensen, E. Garrido, D. V. Fedorov, and H. O. U. Fynbo, *Momentum distributions of particles from decaying low-lying ^{12}C resonances*, Phys. Rev. **C 77**, 064305 (2008).
- [26] H. O. U. Fynbo, R. Álvarez-Rodríguez, A. S. Jensen, O. S. Kirsebom, and D. V. Fedorov, E. Garrido, *Three-body decays and R-matrix analyses*, Phys. Rev. **C 79**, 054009 (2009).
- [27] D. M. Brink, *The Alpha-Particle Model of Light Nuclei*, in Proc. Int. School of Physics “Enrico Fermi”, Course XXXVI, Varenna, 1965 ed C Bloch (New York: Academic Press), 1966, p. 247.
- [28] D. L. Hill and J. A. Wheeler, *Nuclear Constitution and the Interpretation of Fission Phenomena*, Phys. Rev. **89**, 1106 (1953).
- [29] E. Uegaki, S. Okabe, Y. Abe, and H. Tanaka, *Structure of the Excited States in ^{12}C . I*, Prog. Theo. Phys. **57**, 1262-1276 (1977).
- [30] E. Uegaki, Y. Abe, S. Okabe, and H. Tanaka, *Structure of the Excited States in ^{12}C .II*, Prog. Theo. Phys. **62**, 1621-1640 (1979).
- [31] M. Kamimura, T Matsuse and K. Takada, *New Analytical Derivation of Kernels in the Resonating Group Method for Composite-Particle Scattering and Molecule-Like Structures*, Prog. Theo. Phys. **47**, 1537 (1972).
- [32] M. Kamimura and T Matsuse *New Analytical Derivation of Kernels in the Resonating Group Method for Composite-Particle Scattering and Molecule-Like Structures*, Prog. Theo. Phys. **51**, 438 (1974).
- [33] M. Kamimura, *Transition Densities between the $0_1^+, 2_1^+, 4_1^+, 0_2^+, 2_2^+, 1_1^-$, and 3_1^- States in ^{12}C derived from the 3-alpha Resonating-Group Wave-Functions*, Nucl. Phys. **A351**, 456-480 (1981).
- [34] H. Horiuchi, *Many-Vluster Problem by the Orthoigonal-ity Condition Model*, Prog. Theo. Phys. **51**, 1266 (1974); **53**, 447 (1975).
- [35] Y. Funaki, H. Horiuchi, P. Schuck, G. Ropke, Eur. Phys. Jour. **A 24**, 321 (2005).
- [36] Y. Funaki, H. Horiuchi, W. von Oertzen, G. Ropke, P. Schuck, A. Tohsaki, and T. Yamada, *Concepts of nuclear α -particle condensation*, Phys. Rev. C **80**, 064326 (2009), and references therein, M. Kamimura, Nucl. Phys. **A351**, 456 (1981).

- [37] A. Tohsaki, H. Horiuchi, P. Schuck, and G. Röpke, *Alpha-Particle Condensation in C-12 and O-16*, Phys. Rev. Lett. **87**, 192501 (2001).
- [38] S.G. Nilsson, *Binding States of Individual Nucleons in Strongly Deformed Nuclei*, Mat. Fys. Medd., Dan. Vid. Selsk. **29** (1955).
- [39] C. Y. Wong, *Shells in a Simple Anisotropic Harmonic Oscillator*, Phys. Lett. **62B**, 668-671 (1970).
- [40] R. Bijker and F. Iachello, *Cluster States in Nuclei as Representations of a $U(+1)$ Group*, Phys. Rev. C **61**, 067305 (2000).
- [41] R. Bijker and F. Iachello, *The Algebraic Cluster Model: Three-Body Clusters*, Ann. Phys. (N.Y.) **298**, 334 (2002).
- [42] D.J. Marín-Lambarri, R. Bijker, M. Freer, M. Gai, Tz. Kokalova, D.J. Parker, and C. Wheldon, *Evidence for Triangular D_{3h} Symmetry in ^{12}C* , Phys. Rev. Lett. **113**, 012502 (2014).
- [43] W. von Oertzen, Z. Phys. **A 354**, 37 (1996); W. von Oertzen, M. Freer and Y. Kanada-Enyo, Phys. Rep. **432**, 43 (2006).
- [44] Y. Kanada-Enyo, *Variation after Angular Momentum Projection for the Study of Excited States Based on Antisymmetrized Molecular Dynamics*, Phys. Rev. Lett. **81**, 5291 (1998).
- [45] Y. Kanada-Enyo and H. Horiuchi, *Structure of Light Unstable Nuclei Studied with Antisymmetrized Molecular Dynamics*, Prog. of Theo. Phys. Suppl. **142** 205 (2001).
- [46] Y. Kanada-Enyo, *The Structure of Ground and Excited States of ^{12}C* , Prog. of Theo. Phys. **117** 655 (2007).
- [47] R. Roth, T. Neff, H. Hergert and H. Feldmeier, Nucl. Phys. **A 745**, 3 (2004).
- [48] M. Chernykh, H. Feldmeier, T. Neff, P. von Neumann-Cosel, and A. Richter, *Structure of the Hoyle State in ^{12}C* , Phys. Rev. Lett. **98**, 032501 (2007).
- [49] R. Roth, J. Langhammer, A. Calci, S. Binder, and P. Navratil, *Similarity-Transformed Chiral $NN+3N$ Interactions for the Ab Initio Description of ^{12}C and ^{16}O* , Phys. Rev. Lett. **107**, 072501 (2011).
- [50] B.R. Barrett, P. Navratil and J.P. Vary, Prog. Part. Nucl. Phys. **69**, 131 (2013).
- [51] A. C. Dreyfuss, K. D. Launey, T. Dytrych, J. P. Draayer, and C. Bahri, *Hoyle state and rotational features in Carbon-12 within a no-core shell model framework*, Phys. Lett. **B 727**, (2013), pp. 511-515.
- [52] E. Epelbaum, H. Krebs, D. Lee, and U.-G. Meissner, *Ab Initio Calculation of the Hoyle State*, Phys. Rev. Lett. **106**, 192501 (2011).
- [53] J. L. Egido and L. M. Robledo, Nucl. Phys. **A 738**, 31 (2004).
- [54] P. Arumugam, B.K. Sharma, S.K. Patra, R.K. Gupta, Phys. Rev. **C 71**, 064308 (2005).
- [55] P.-G. Reinhard, J. A. Maruhn, A. S. Umar, and V. E. Oberacker, Phys. Rev. **C 83**, 034312 (2011).
- [56] J.-P. Ebran, E. Khan, T. Niki, and D. Vretenar, *How atomic nuclei cluster*, Nature **487**, 341 (2012); J.-P. Ebran, E. Khan, T. Niki, and D. Vretenar, *Density functional theory studies of cluster states in nuclei*, Phys. Rev. **C 90**, 054329 (2014); J.-P. Ebran, E. Khan, T. Niki, and D. Vretenar, *Jour. Phys. G* **44**, 103001 (2017).
- [57] T. Ichikawa, J. A. Maruhn, N. Itagaki, and S. Ohkubo, Phys. Rev. Lett. **107**, 112501 (2011); Y. Iwata, T. Ichikawa, N. Itagaki, J. A. Maruhn, and T. Otsuka, Phys. Rev. **C 92**, 011303 (2015); J. M. Yao, N. Itagaki, and J. Meng, Phys. Rev. **C 90**, 054307 (2014).
- [58] P. W. Zhao, N. Itagaki, and J. Meng, Phys. Rev. Lett. **115**, 022501 (2015); E. F. Zhou, J. Yao, Z. Li, J. Meng, and P. Ring, Phys. Lett. **B 753**, 227 (2016);
- [59] A. V. Afanasjev and H. Abusara, Phys. Rev. **C 97**, 024329 (2018).
- [60] A. Staszczak and C. Y. Wong, (to be published).
- [61] Y. Suzuki, H. Horiuchi, and K. Ikeda, Prog. Theor. Phys. **47**, 1517 (1972).
- [62] Z. X. Ren, S. Q. Zhang, P. W. Zhao, N. Itagaki, J. A. Maruhn, and J. Meng, *Stability of the Linear Chain Structure for ^{12}C in Covariant Density Functional Theory on a 3D Lattice* Sci.China Phys.Mech.Astron.**62**, 112062 (2019) [arXiv:1805.07901].
- [63] T. Inakura and S. Mizutori, *Rod-shaped rotational states in $N=Z$ even-even nuclei from ^{12}C to ^{32}S* , Phys. Rev. **C 98**, 044312 (2018).
- [64] J. A. Wheeler, *Nucleonics Notebook*, 1950 (unpublished), see also p. 297 in G. Gamow, *Biography of Physics*, Harper & Brothers Publishers, N.Y. 1961; Princeton University Graduate Course Physics 576 Take-Home Examination Problem 2, May 22, 1963 (unpublished).
- [65] J. A. Wheeler and K. Ford, *Geons, Black Holes, and Quantum Foam*, W. W. Norton & Company, New York 1998, page 232.
- [66] C. Y. Wong, *Toroidal Nuclei*, Phys. Lett. **41B**, 446-450 (1972)
- [67] C. Y. Wong, *Toroidal and Spherical Bubble Nuclei*, Ann. of Phys. (N.Y.) **77**, 279 (1973).
- [68] M. Brack, J. Damgaard, A. S. Jensen, H. C. Pauli, V. Strutinsky, and C. Y. Wong, *Funny Hills: The Shell-Correction Approach to Nuclear Shell Effects and Its Applications to the Fission Process*, Rev. Mod. Phys. **44**, 320-405 (1973).
- [69] A. Staszczak and C. Y. Wong, *A Region of High-Spin Toroidal Isomers*, Phys.Lett. **B 738**, 401-404 (2014), [arXiv:1312.3413].
- [70] X. G. Cao, E. J. Kim, K. Schmidt, K. Hagel, M. Barbui, J. Gauthier, S. Wuenschel, G. Giuliani, M. R. D. Rodriguez, S. Kowalski, H. Zheng, M. Huang, A. Bonasera, R. Wada, N. Blando, G. Q. Zhang, C. Y. Wong, A. Staszczak, Z. X. Ren, Y. K. Wang, S. Q. Zhang, J. Meng, and J. B. Natowitz, *Examination of Evidence for Resonances at High Excitation Energy in the 7α Disassembly of ^{28}Si* , Phys. Rev. **C 99**, 014606 (2019), arxiv:1801.07366.
- [71] Wei Zhang, Hao-Zhao Liang, Shuang-Quan Zhang, Jie Meng, *Search for Ring-Like Nuclei under Extreme Conditions*, Chin. Phys. Lett., **27**, 102103 (2010).
- [72] T. Ichikawa *et al.*, *Existence of exotic torus configuration in high-spin excited states of ^{40}Ca* , Phys.Rev.Lett. **109** (2012) 232503; T. Ichikawa *et al.*, *Pure collective precession motion of a high-spin torus isomer*, Phys.Rev. **C90**, 034314 (2014).
- [73] T. Ichikawa, K. Matsuyanagi, J. A. Maruhn, N. Itagaki, *High-spin torus isomers and their precession motions* Phys.Rev. **C90**, 034314 (2014).
- [74] A. Staszczak and C. Y. Wong, *Particle-hole Nature of the Light High-spin Toroidal Isomers*, Acta Phys.Polon. **B46**, no.3, 675 (2015); arXiv:1504.07646 [nucl-th]
- [75] A. Staszczak and C. Y. Wong, *Toroidal High-Spin Isomers in Light Nuclei with N not equal to Z* , Phys.Scripta **90**, (2015) 114006; arXiv:1412.0050 [nucl-th]
- [76] A. Staszczak and C. Y. Wong, *Theoretical Studies of Possible Toroidal High-Spin Isomers in the Light-*

- Mass Region*, EPJ Web Conf. **117**, 04008 (2016), arXiv:1510.04610.
- [77] G. A. Grin, C. Joseph, C. Y. Wong, and T. Tamura, *Scattering of 14.1 MeV Neutrons from ^{12}C* , Phys. Lett. **25B**, 387 (1967).
 - [78] D. Vautherin and D. Brink, *Hatree-Fock Calculations with Skyrme's Interaction. I. Spherical Nuclei*, Phys. Rev. **C5**, 626 (1972).
 - [79] D. Vautherin and D. Brink, *Hatree-Fock Calculations with Skyrme's Interaction. II. Axially Deformed Nuclei*, Phys. Rev. **C7**, 296 (1973).
 - [80] J. Bartel, P. Quentin, M. Brack, C. Guet, H.B. Håkansson, Nucl. Phys. A **386** (1982) 79-100.
 - [81] K. Hara and Y. Sun, *Projected Shell Model and High Spin-Spectroscopy*, Int. J. Mod. Phys. **E 4**, 637 (1995).
 - [82] Y. Sun and C. L. Wu, *Multishell Shell Model for Heavy Nuclei*, Physical Review **C 68**, 024315 (2003).
 - [83] Y. Sun, *Projected Shell Model Study on Nuclei Near the $N=Z$ Line*, Eur. Phys. J. **A20**, 133-138 (2004), arXiv:nucl-th/0211043v2.
 - [84] Y. Sun, *Projected Shell Model Description for Nuclear Isomers*, Rev. Mex. Fis. Suppl. **54**, 01122 (2008), arXiv:0803.1700 [nucl-th]
 - [85] M. Alcorta, O. Kirsebom, M.J.G. Borge, H.O.U. Fynbo, K. Riisager, O. Tengblad, *A Complete Kinematics Approach to study Multi-Particle Final State Reactions*, Nucl. Instrum. Methods **A 605**, 318 (2009).
 - [86] M. Freer, S. Almaraz-Calderon, A. Aprahamian, N. I. Ashwood, M. Barr, B. Bucher, P. Copp, M. Couder, N. Curtis, X. Fang, F. Jung, S. Leshner, W. Lu, J. D. Malcolm, A. Roberts, W. P. Tan, C. Wheldon, and V. A. Zisman *Evidence for a New ^{12}C State at 13.3 MeV*, Phys. Rev. **C 83**, 034314 (2011).
 - [87] E. Garrido, A.S. Jensen, D.V. Fedorov, *Three-body Bremsstrahlung and the Rotational Character of the ^{12}C -Spectrum*, Phys. Rev. **C91**, 054003 (2015)
 - [88] C. Y. Wong and A. Staszczak, *Shells in Toroidal Nuclei in the Intermediate Mass Region*, Phys. Rev. **C98**, 034316 (2018).
 - [89] A. Kosior, A. Staszczak, C. Y. Wong, *Superheavy Toroidal nuclei in the Skyrme Energy Functional Framework*, Acta Phys. Pol. B Proc. Suppl. **10**, 249 (2017), [arXiv:1701.06327]
 - [90] A. Staszczak, C. Y. Wong, A. Kosior, *Toroidal High-Spin Isomers in the Nucleus $^{304}120$* Phys. Rev. **C 95**, 054315 (2017) [arXiv:1705.01408]
 - [91] M. Abramowitz and I. A. Stegun, *Handbook of Mathematical Functions*, Dover Publications, N.Y. 1965.
 - [92] A. N. Danilov, T. L. Belyaeva, A. S. Demyanova, S. A. Goncharov, and A. A. Ogloblin, *Determination of Nuclear Radii for Unstable States in ^{12}C with Diffraction Inelastic Scattering*, Phys. Rev. **C80**, 054603 (2009).
 - [93] S. Ali, A. R. Bodmer, *Phenomenological - potentials*, Nucl. Phys. **80**, 99 (1966).
 - [94] D. Kolb and C. Y. Wong, *Shape Isomersism in Mercury Isotopes*, Nucl. Phys. **A245**, 205-220, (1975).
 - [95] K. W. Ford, D. L. Hill, M. Wakano, J. A. Wheeler, *Quantum Effects near a Barrier Maximum*, Ann. Phys. **7**, 230-258 (1959).
 - [96] C. Y. Wong and J. Bang, *Penetration through a Double Barrier*, Phys. Lett. **B30**, 61 (1969).
 - [97] O. S. Kirsebom, *Decay of $^{12}\text{C}^*$ into three α particles*, Few-Body Syst. **54**, 755 (2013).